



Molecular antagonism between X-chromosome and autosome signals determines nematode sex

Behnom Farboud, Paola Nix, Margaret M. Jow, et al.

Genes Dev. 2013 27: 1159-1178 originally published online May 10, 2013

Access the most recent version at doi:[10.1101/gad.217026.113](https://doi.org/10.1101/gad.217026.113)

Supplemental Material

<http://genesdev.cshlp.org/content/suppl/2013/05/02/gad.217026.113.DC1.html>

References

This article cites 64 articles, 35 of which can be accessed free at:
<http://genesdev.cshlp.org/content/27/10/1159.full.html#ref-list-1>

Email alerting service

Receive free email alerts when new articles cite this article - sign up in the box at the top right corner of the article or [click here](#)



ChIP-seq with just 10,000 cells!
Apply for our new ChIP-seq grant



diagenode
Innovating Epigenetic Solutions

To subscribe to *Genes & Development* go to:
<http://genesdev.cshlp.org/subscriptions>

Molecular antagonism between X-chromosome and autosome signals determines nematode sex

Behnom Farboud,¹ Paola Nix,^{1,2} Margaret M. Jow,^{1,3} John M. Gladden,^{1,4} and Barbara J. Meyer^{1,5}

¹Howard Hughes Medical Institute, Department of Molecular and Cell Biology, University of California at Berkeley, Berkeley, California 94720, USA

Sex is determined in *Caenorhabditis elegans* by the ratio of X chromosomes to the sets of autosomes, the X:A signal. A set of genes called X signal elements (XSEs) communicates X-chromosome dose by repressing the masculinizing sex determination switch gene *xol-1* (XO lethal) in a dose-dependent manner. *xol-1* is active in 1X:2A embryos (males) but repressed in 2X:2A embryos (hermaphrodites). Here we showed that the autosome dose is communicated by a set of autosomal signal elements (ASEs) that act in a cumulative, dose-dependent manner to counter XSEs by stimulating *xol-1* transcription. We identified new ASEs and explored the biochemical basis by which ASEs antagonize XSEs to determine sex. Multiple antagonistic molecular interactions carried out on a single promoter explain how different X:A values elicit different sexual fates. XSEs (nuclear receptors and homeodomain proteins) and ASEs (T-box and zinc finger proteins) bind directly to several sites on *xol-1* to counteract each other's activities and thereby regulate *xol-1* transcription. Disrupting ASE- and XSE-binding sites in vivo recapitulated the misregulation of *xol-1* transcription caused by disrupting cognate signal element genes. XSE- and ASE-binding sites are distinct and nonoverlapping, suggesting that direct competition for *xol-1* binding is not how XSEs counter ASEs. Instead, XSEs likely antagonize ASEs by recruiting cofactors with reciprocal activities that induce opposite transcriptional states. Most ASE- and XSE-binding sites overlap *xol-1*'s -1 nucleosome, which carries activating chromatin marks only when *xol-1* is turned on. Coactivators and corepressors tethered by proteins similar to ASEs and XSEs are known to deposit and remove such marks. The concept of a sex signal comprising competing XSEs and ASEs arose as a theory for fruit flies a century ago. Ironically, while the recent work of others showed that the fly sex signal does not fit this simple paradigm, our work shows that the worm signal does.

[**Keywords:** sex determination; haploinsufficiency; dose-sensitive signals; dosage compensation; nuclear hormone receptor; T-box protein]

Supplemental material is available for this article.

Received March 3, 2013; revised version accepted April 15, 2013.

Dose-dependent signals play essential roles in cell fate decisions during development. Small differences in the concentrations of key regulatory molecules are translated into dramatically different developmental fates (Herskowitz 1989; Perry et al. 2009; Shilo et al. 2013). A prime example is sex determination (Bull 1983; Charlesworth and Mank 2010). In many species, sex is determined by a chromosome-counting mechanism that tallies the number of X chromosomes relative to the ploidy,

the sets of autosomes. The molecular strategies for such X:A-counting mechanisms have been difficult to dissect. For both the nematode *Caenorhabditis elegans* and the fruit fly *Drosophila melanogaster*, an X:A signal of 0.5 (1X:2A) elicits male fate, while a signal of 1.0 (2X:2A) elicits female (or hermaphrodite) fate (Bridges 1921; Nigon 1951). Worms discriminate with high fidelity between even smaller differences in the X:A signal: 2X:3A (0.67) embryos develop into fertile males, while 3X:4A (0.75) embryos develop into fertile hermaphrodites (Madl and Herman 1979). Neither the components of the worm sex signal nor its mechanism for determining sex are well understood. Particularly elusive has been how X and autosomal signals oppose one another to communicate the relative doses of X chromosomes and autosomes.

The initial concept that sex can be determined through an X:A-sensing mechanism emerged from Calvin Bridges' (Bridges 1921) extensive analysis of fly sexual fates induced

Present addresses: ²Department of Biology, University of Utah, Salt Lake City, UT 84112, USA; ³Department of Biology, San Francisco State University, San Francisco, CA 94132, USA; ⁴Bioengineering and Biomass Science, Conversion Technology Department, Sandia National Laboratories, Livermore, CA 94551, USA.

⁵Corresponding author

E-mail bjmeyer@berkeley.edu

Article published online ahead of print. Article and publication date are online at <http://www.genesdev.org/cgi/doi/10.1101/gad.217026.113>.

by different X:A values. In 1921, he proposed that the fly sex signal is composed of a set of feminizing genes on X and an antagonistic set of masculinizing genes on autosomes. Sex would be determined by the ratio of these opposing factors. His hypothesis met wide acceptance and was presented in textbooks as fact without validation by the discovery of such antagonistic sex-determining genes. Ironically, detailed molecular analysis conducted decades later showed that the fly X:A sex determination signal does not fit this elegant textbook paradigm (Erickson and Quintero 2007), but we show here that the worm signal does.

In flies, a set of feminizing genes on X called X signal elements (XSEs) communicates X-chromosome number (Cline 1988; Erickson and Cline 1991, 1993; Sefton et al. 2000; Salz and Erickson 2010), but ploidy appears not to be signaled by a corresponding set of masculinizing autosomal genes (Erickson and Quintero 2007). Only a single autosomal signal element (ASE) has been identified through extensive genetic screens (Barbash and Cline 1995). That ASE influences sex determination only weakly and is thought to function relatively late to fine-tune the counting process. The effect of ploidy in this dose-sensitive process was recently shown to be indirect (Erickson and Quintero 2007).

In *C. elegans*, X-chromosome number is also communicated by a set of *trans*-acting XSEs encoded on X chromosomes (Fig. 1A; Akerib and Meyer 1994; Hodgkin et al. 1994; Nicoll et al. 1997; Carmi et al. 1998; Gladden and Meyer 2007; Gladden et al. 2007; Meyer 2010). XSEs act in a cumulative, dose-dependent manner to repress the masculinizing sex determination switch gene called *xol-1* (XO lethal) in 2X:2A embryos. *xol-1* encodes a GHMP kinase family member that induces the male fate when active and permits the hermaphrodite fate when inactive (Miller et al. 1988; Rhind et al. 1995; Luz et al. 2003). *xol-1* also controls the level of X-linked gene expression, and hence viability, by regulating the process of X-chromosome dosage compensation (Miller et al. 1988; Chuang et al. 1994; Rhind et al. 1995; Dawes et al. 1999). *xol-1* coordinately regulates both sex determination and dosage compensation by negatively regulating the feminizing switch gene *sdv-2* (sex determination and dosage compensation), which triggers assembly of all dosage compensation complex (DCC) subunits onto both X chromosomes of XX embryos to reduce X-linked gene expression by half (Dawes et al. 1999; Pferdehirt et al. 2011). *sdv-2* also induces hermaphrodite sexual differentiation by repressing the autosomal male sex-determining gene *her-1*. Inappropriate repression of *xol-1* in 1X:2A embryos or inappropriate activation of *xol-1* in 2X:2A embryos causes embryonic lethality due to misregulation of the DCC and hence incorrect levels of X-chromosome gene expression.

XSEs were discovered through genetic schemes that identified suppressors of the lethal effects caused by *xol-1* misregulation (Akerib and Meyer 1994; Hodgkin et al. 1994; Nicoll et al. 1997; Carmi et al. 1998; Gladden and Meyer 2007). XSEs control *xol-1* at two distinct levels: transcriptional repression via the nuclear receptor SEX-1 and the ONECUT homeodomain protein CEH-39 and

post-transcriptional repression via the RNA-binding protein FOX-1 (Hodgkin et al. 1994; Nicoll et al. 1997; Carmi et al. 1998; Skipper et al. 1999; Gladden and Meyer 2007; Gladden et al. 2007). Disruption of SEX-1 causes extensive but incomplete XX-specific lethality, and simultaneous disruption of both SEX-1 and CEH-39 or SEX-1 and FOX-1 causes complete XX lethality due to derepression of *xol-1*. Disruption of either CEH-39 or FOX-1 alone has minimal effects on viability. Transcriptional repression is the predominant form of *xol-1* regulation, but prior to our current study, it was not known whether SEX-1 and CEH-39 control *xol-1* indirectly or through direct molecular interactions with *cis*-acting regulatory regions.

Our previous work showed that the autosomal signal includes a *trans*-acting ASE that counters XSEs in part to coordinately regulate both sex determination and dosage compensation by activating *xol-1* (Fig. 1A; Powell et al. 2005). This ASE, called SEA-1 (signal element on autosome), was identified as a suppressor of the XX-specific lethality caused by loss of XSEs. SEA-1 is T-box transcription factor that acts in a dose-dependent manner to stimulate *xol-1* transcription. Not known was whether SEA-1 acts directly on *xol-1* to control its expression, how an ASE might antagonize XSEs, and whether worms, like flies, have only a single weak ASE and also use an ASE-independent mechanism to communicate ploidy.

In our current study to dissect the *C. elegans* sex determination signal and discover the molecular mechanisms by which small differences in the X:A signal elicit alternate sexual fates, we first conducted a genetic screen to identify additional ASEs and then explored the biochemical basis by which XSEs counter ASEs to determine sex. We show here that ploidy is communicated by multiple discrete ASEs, which function in a dose-dependent and cumulative manner to activate *xol-1* transcription, consistent with Bridges' hypothesis for flies (Bridges 1921). We also show that XSEs engage in molecular rivalry with ASEs to overcome their activating effects, thereby translating the twofold difference in X-chromosome dose between the sexes into the high or low activity state of *xol-1*. Transcriptional activation of *xol-1* by ASEs is direct. Two of the ASEs, SEA-1 and SEA-2 (a zinc finger protein), bind to multiple sites within *xol-1*. Transcriptional repression by XSEs is similarly direct: SEX-1 and CEH-39 also bind to numerous *xol-1* sites in vitro. Disrupting these ASE- and XSE-binding sites in vivo recapitulates the deregulation of *xol-1* expression caused by disrupting the corresponding signal element genes. The known XSE- and ASE-binding sites are distinct and nonoverlapping, suggesting that direct competition for binding to *xol-1* is unlikely to be the mechanism by which XSEs oppose ASEs. Since other T-box proteins, nuclear receptors, and homeobox proteins tether coactivators or corepressors to specific binding sites (Asahara et al. 1999; Privalsky 2004; Murakami et al. 2005), the most plausible model is that XSEs and ASEs antagonize each other by recruiting cofactors with reciprocal activities that induce opposite transcriptional states. In summary, we demonstrated that multiple, antagonistic molecular interactions carried out on

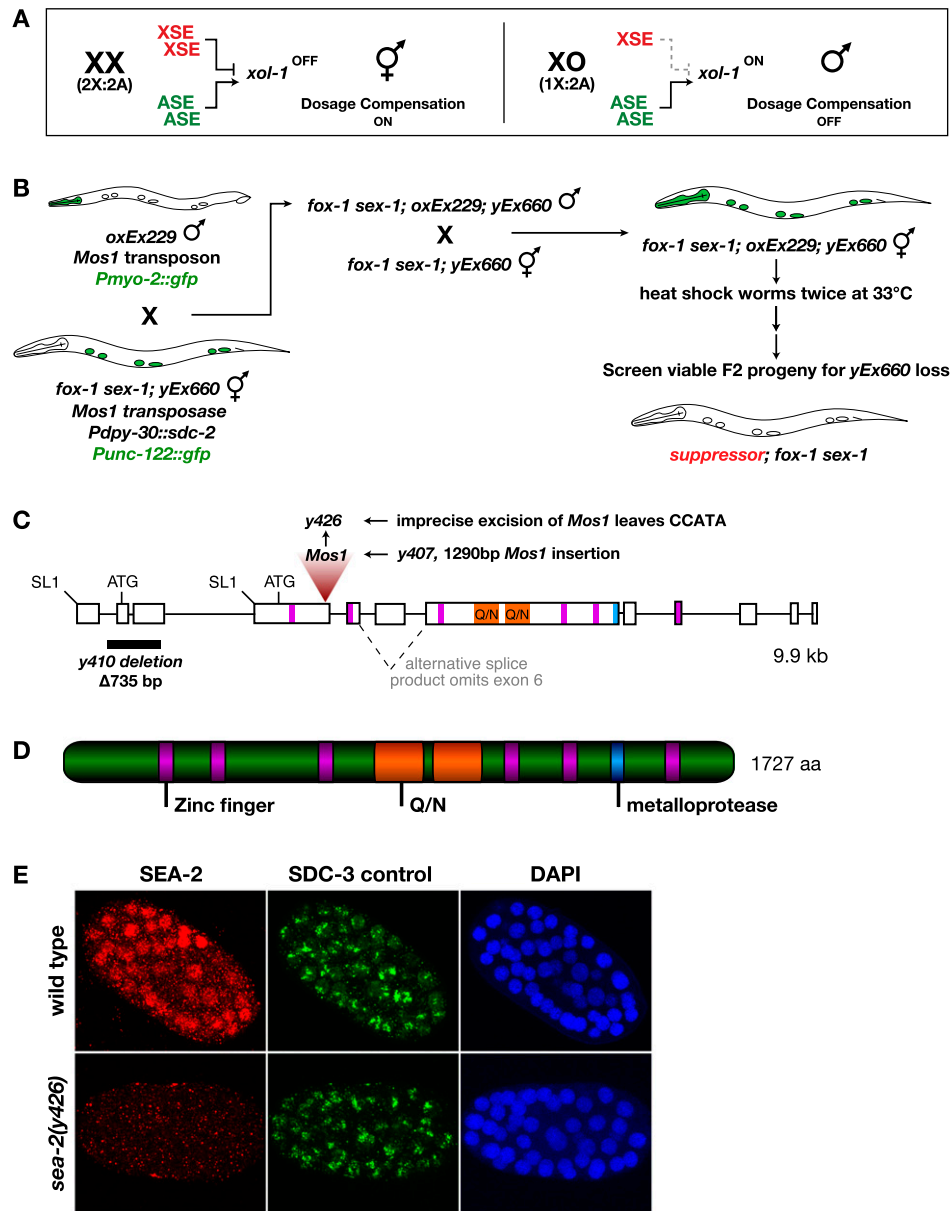


Figure 1. Identification of an ASE that encodes a zinc finger protein with Q/N and metalloprotease repeats. (A) Regulation of *xol-1* by XSEs and ASEs. In diploid XX embryos (2X:2A), the double dose of XSEs outcompetes the double dose of ASEs to repress *xol-1*, thereby activating the hermaphrodite-specific gene *sdc-2* and turning on dosage compensation and the hermaphrodite program of sexual differentiation. *sdc-2* activates dosage compensation by triggering binding of the DCC to both X chromosomes, where it turns down X-chromosome expression by about half. In diploid XO embryos (1X:2A), the single dose of XSEs fails to overcome the double dose of ASEs. *xol-1* remains active, represses *sdc-2*, turns on the male program of sexual differentiation, and precludes binding of the DCC to X. (B) Genetic strategy for identifying ASEs. The *Mos1* transposon strain used to obtain suppressors of the XX-specific lethality caused by disrupting two XSEs—*fox-1* and *sex-1*—was made from crosses (shown) involving two initial strains. (1) A *fox-1 sex-1* double-mutant strain carried an extrachromosomal array (*yEx660*) containing three transgenes: the *Mos1* transposase controlled by a heat-shock promoter (*hsp-16-48::Mos1* transposase); *Pdpy-30::sdc-2*, used to suppress the lethality of *fox-1 sex-1* mutants; and *Punc-122::gfp*, a reporter for the array that causes coelomocytes to fluoresce green. (2) The strain carried an extrachromosomal array (*oxEx229*) bearing the *Mos1* transposon and the reporter *Pmyo-2::gfp*, which causes the pharynx to fluoresce green. *Mos1* was mobilized in the final strain (*fox-1 sex-1; oxEx229; yEx660*) by heat shock, and homozygous suppressors were identified among their F2 self progeny as viable hermaphrodites that lacked the *yEx660* array. (C) Structure of the *sea-2* gene showing intron–exon boundaries, locations, and molecular identity of *sea-2* mutations; two SL1 TSL sites; an alternative splice junction; and locations of sequences encoding zinc fingers (magenta), Q/N repeats (orange), and the metalloprotease domain (blue). (D) Schematic of the SEA-2 protein showing locations of zinc fingers, Q/N repeats, and metalloprotease domain. (E) Immunofluorescence images of wild-type and *sea-2(y426)*-null XX embryos stained with the DNA dye DAPI (blue) and antibodies to both SEA-2 (red) and the X-bound dosage compensation protein SDC-3 (green) used as a staining control. The diffuse nuclear SEA-2 signal was eliminated by the *sea-2(y426)*-null mutation, showing antibody specificity.

a single promoter form the basis of the primary sex determination decision in *C. elegans*. This antagonism makes the sex determination process highly responsive to the relative dose of X chromosomes and autosomes so that even tiny changes in the X:A signal elicit different sexual fates.

Results

A Mos1 transposon screen identified an ASE

To identify ASEs, we conducted a genetic screen for mutations that suppressed the hermaphrodite-specific lethality caused by disrupting two XSEs: *fox-1* and *sex-1* (Fig. 1B). Reducing the dose of ASEs in an XSE-deficient XX mutant was expected to restore the X:A balance and thereby re-establish dosage compensation and hermaphrodite viability (Powell et al. 2005). The screen was designed to recover both dominant and recessive mutations. The *Mos1* transposon was used as the mutagen to permit facile molecular identification of disrupted genes (Bessereau et al. 2001).

One strong candidate emerged from analysis of 9400 *Mos1* mutagenized haploid genomes, and three initial experiments suggested that the *Mos1*-disrupted gene encodes an ASE. First, the *y407* suppressor allele restored the viability of *fox-1 sex-1* XX mutants to 36% (Fig. 2B). Inverse PCR of *y407* revealed a *Mos1* insertion site within the ORF K10G6.3, and RNAi against K10G6.3 restored the viability of *fox-1 sex-1* XX mutants to 27%, a level equivalent to *y407*. Second, a deletion allele of K10G6.3 (*y410*) obtained through a directed PCR screen of our *C. elegans* deletion library also restored the viability of *fox-1 sex-1* XX mutants to an equivalent level (24%) (Fig. 2B). XX and XO animals carrying either mutant allele of K10G6.3 were viable. Third, an extrachromosomal array bearing the cosmid encoding K10G6.3 reduced the viability of *y407*; *fox-1 sex-1* XX animals to that of *fox-1 sex-1* XX animals (Materials and Methods). We named the K10G6.3 gene *sea-2* to reflect its likely role in sex determination.

sea-2 encodes a zinc finger protein with glutamine/asparagine-rich repeats

Multiple *sea-2* mRNAs are made by different combinations of two alternative SL1 *trans*-splice acceptor sites at the 5' end and an alternative splice acceptor that eliminates the sixth exon (Fig. 1C). The longest *sea-2* mRNA spans a 9.9-kb genomic region encoding a PQN (prion-like, Q/N-rich) family member of 1727 amino acids (Fig. 1D). SEA-2 also contains six separated zinc finger domains and a metalloprotease motif.

Molecular analysis of *sea-2* mutants revealed that neither *sea-2* allele is null. For *y407*, the *Mos1* insertion resides in exon 4 and is predicted to cause premature termination of translation for both *trans*-spliced messages (Fig. 1C). However, *y407* cDNAs showed that *Mos1* was removed from *sea-2* mRNAs through alternative splicing, thereby restoring the reading frame. For *y410*, the deletion eliminates exons 2 and 3 in the first SL1 *trans*-spliced mRNA but fails to disrupt the second SL1

trans-spliced mRNA (Fig. 1C). The *y410* deletion is predicted to cause premature termination of translation for only the first mRNA.

To isolate a *sea-2*-null mutant, we mobilized *Mos1* in *y407* animals and identified an allele (*y426*) in which all but 5 nucleotides (nt) of *Mos1* had been excised (Fig. 1C). The remaining insertion created a premature translational stop codon and the consequent degradation of both SL1 *trans*-spliced mRNAs (Supplemental Fig. S1). Consistent with *y426* being a null allele, *y426* increases the viability of *fox-1 sex-1* mutants to 50%, a level greater than that achieved by either *y407* or *y410* (Fig. 2B).

SEA-2 accumulates in nuclei of young embryos during sex determination

Immunofluorescence experiments with SEA-2 antibodies showed diffuse nuclear accumulation of SEA-2 in embryos of the 20- to 30-cell stage (Fig. 1E), when sex determination begins, and greatly diminished nuclear levels of SEA-2 in embryos beyond the 200-cell stage, after dosage compensation is established (data not shown). SEA-2 antibody staining was present at low levels in *y407* mutants and absent in *y426*-null mutants (Fig. 1E), confirming the specificity of the SEA-2 antibody and the molecular and genetic characterization of the mutants.

Similar nuclear localization and timing of accumulation were observed for the XSE proteins and the ASE SEA-1 (Nicoll et al. 1997; Carmi et al. 1998; Powell et al. 2005; Gladden and Meyer 2007), further implying an early role for SEA-2 in sex determination. The nuclear localization of the zinc finger SEA-2 protein and the presence of PQN protein-protein interaction motifs suggests that SEA-2 acts as a transcription factor that associates with other proteins to achieve transcriptional regulation (Michelitsch and Weissman 2000; Wolfe et al. 2000).

SEA-2 is a bona fide ASE

To be classified as a bona fide ASE, a gene must fulfill several genetic criteria. First, reducing the dose of an ASE should suppress the XX lethality caused by reducing the dose of XSEs and enhance the XO lethality caused by increasing the dose of XSEs. Second, increasing the dose of an ASE should enhance the XX lethality caused by reducing the dose of XSEs and suppress the XO lethality caused by increasing the dose of XSEs. In fulfilling both criteria, an ASE should act in a dose-dependent manner in the early zygote, the developmental stage in which the X:A signal is assessed to determine sexual fate.

sea-2 meets all of the criteria for an ASE. First, *sea-2* loss-of-function alleles suppress not only the synergistic XX lethality of the *fox-1 sex-1(y263)* double mutant, but also the XX lethality of the *sex-1(y424)*-null mutant (from 20% viability to 34%; $P < 0.001$) and the synergistic XX lethality of the *sex-2(y324) sex-1(y263)* double mutant (from 0% viability to 38%; $P < 0.001$) (Fig. 2B). The suppression is dose-dependent: The heterozygous *sea-2(y407)/+* mutation restores viability of *fox-1 sex-1(y263)* mutants to 13%, and the homozygous *sea-2(y407)* mutation restores viability to 36% ($P < 0.001$) (Fig. 2B).

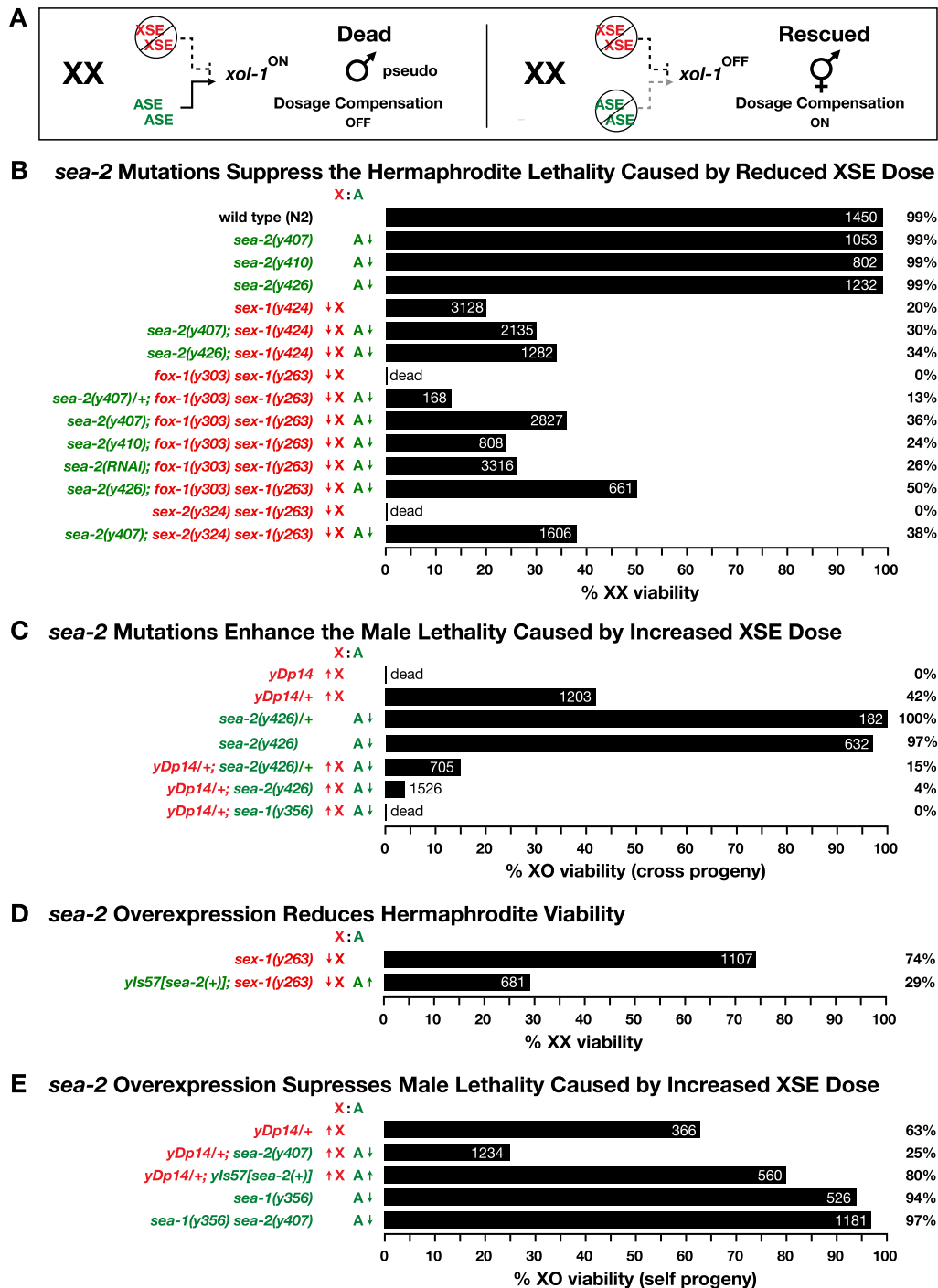


Figure 2. *sea-2* fulfills the genetic criteria for an ASE. (A) Genetic properties of XSEs and ASEs in XX animals. Reducing the dose of XSEs causes *xol-1* activation and the consequent masculinization and death of XX animals. Reducing the dose of ASEs in these XSE-deficient XX animals restores the X:A signal, thereby repressing *xol-1* and re-establishing viability. (B–E) Histograms show that *sea-2* fulfills the genetic properties of an ASE with respect to viability. Genotype of animals assayed for viability is shown on the left, the effect of mutation on X or A signal is shown by an arrow (up, increase; down, decrease), the percent adult viability is on the X-axis, and the total number of embryos counted per experiment is given on each line (white). Formulas for adult viability, crosses (when appropriate), and methods for scoring are described in the Materials and Methods. *sea-2* mutations suppress the XX lethality caused by reduced XSE dose (B) and enhance the XO lethality caused by increased XSE dose (C). Elevation of *sea-2* dose reduces XX viability (D) and increases viability of XO animals with elevated XSE dose (E).

Furthermore, *sea-2* loss-of-function mutations increase the XO lethality caused by increasing the dose of XSEs, although *sea-2* mutations alone appear to have no adverse effect on the viability or morphology of XO animals (Fig. 2C). The viability of XO animals with one extra copy of *fox-1* and *ceh-39* carried on the X duplication *yDp14* was reduced from 42% to 15% by *sea-2(y426)/+* and to 4% by homozygous *sea-2(y426)* ($P < 0.001$). Because the *sea-2* mutation was introduced on a paternal chromosome, the enhanced lethality must have been caused by a change in the zygotic dose of *sea-2*.

Second, increasing the dose of *sea-2* suppressed the XO lethality caused by increasing the dose of XSEs and enhanced the XX lethality caused by decreasing the dose of XSEs. Multiple copies of *sea-2(+)* carried on the integrated array *yIs57* increased the viability of *yDp14/+* males from 63% to 80% ($P < 0.001$) (Fig. 2E) and decreased the viability of *sex-1(y263)* XX mutants from 74% to 29% ($P < 0.001$) (Fig. 2D). Together, these results show that *sea-2* is an ASE that counters the action of XSEs to promote the male fate.

ASEs function cumulatively

Analysis of *sea-1* and *sea-2* mutant combinations revealed that the two ASEs act cumulatively to oppose XSEs. The *sea-1(y356) sea-2(y407)* double combination increased the viability of *sex-1(y424)* XX-null mutants from 20% to 77% ($P < 0.001$), while the single *sea-1(y356)* and *sea-2(y407)* mutations increased the viability to only 51% ($P < 0.001$) and 30% ($P < 0.001$), respectively (Fig. 3A). Furthermore, *sea-1* and *sea-2* mutations act together in a dominant fashion to suppress the XX lethality. While the heterozygous *sea-1(y356)/+* mutation failed to increase the viability of *fox-1(y303) sex-1(y263)* mutants (Fig. 3A) and the heterozygous *sea-2(y407)/+* mutation only increased the viability from 0% to 13% ($P < 0.001$) (Fig. 2B), the *trans*-heterozygous *sea-1/sea-2* combination increased the viability to 36% ($P < 0.001$), and the homozygous *sea-1 sea-2* combination increased the viability to 70% ($P < 0.001$) (Fig. 3A).

In reciprocal experiments, increasing the dose of the wild-type *sea-1* and *sea-2* genes decreased the viability of XX animals in a cumulative manner. At 25°C, multiple copies of either *sea-1* (*yIs61*) or *sea-2* (*yIs57*) had only a small effect on XX viability (89% and 98%, respectively), but multiple copies of both reduced the viability of XX animals to 52% ($P < 0.001$) (Fig. 3B). The viability was restored to 93% by a *xol-1* mutation, showing that the XX lethality caused by increased doses of *sea-1* and *sea-2* was due to misregulation of *xol-1* (see Supplemental Fig. S4A for similar experiments conducted at 20°C). Thus, ASEs, like XSEs, function together to communicate the sex signal and act predominantly upstream of *xol-1* to coordinately regulate both sex determination and dosage compensation.

SEA-1 and SEA-2 act together to communicate the autosomal signal but do not comprise the entire signal. Null alleles of neither *sea-1* nor *sea-2* suppressed any of the XX lethality caused by null alleles of both *fox-1(y303)* and *sex-1(y424)*, even though null alleles of either ASE

partially suppressed the synergistic XX lethality caused by the *fox-1(y303)*-null allele and the *sex-1(y263)* partial loss-of-function allele (Fig. 3A). Furthermore, only 17% of *sea-1(y356) sea-2(y426); fox-1(y303) sex-1(y424)* quadruple XX mutants are viable. Thus, while *sea-1* and *sea-2* are important ASEs, they do not constitute the entire autosomal signal (Fig. 3A).

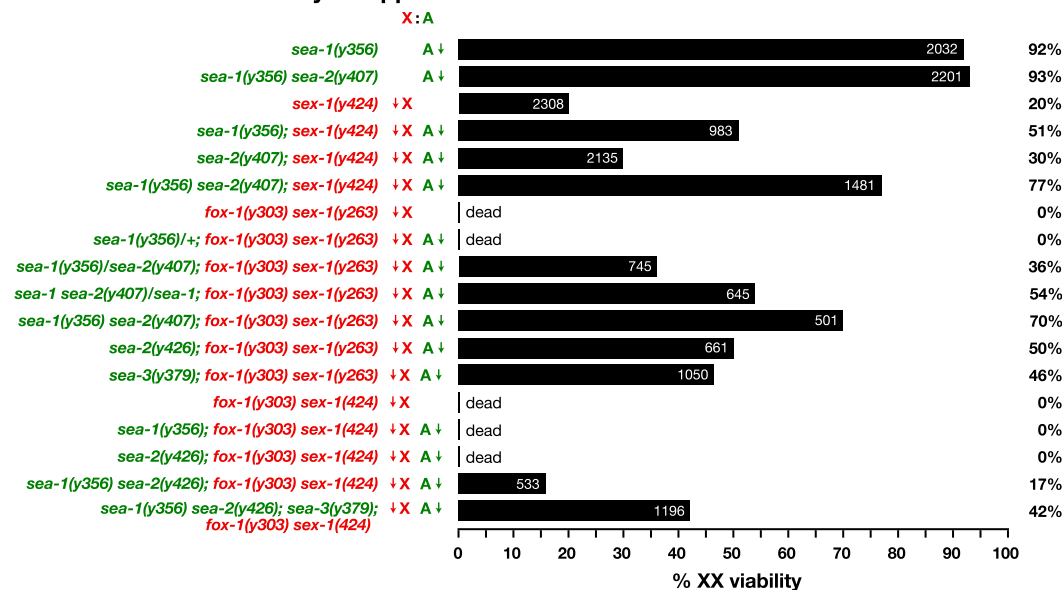
Evidence of additional ASEs came from our finding that the candidate ASE mutation *y379*, which was recovered in an earlier EMS-based genetic screen (Powell et al. 2005) but was not identified molecularly, behaves as a bona fide ASE mutation. We named the gene *sea-3*. The *sea-3(y379)* mutant allele partially suppresses the lethality of *fox-1(y303) sex-1(y263)* mutants and further suppresses the lethality of *fox-1(y303) sex-1(y424)*-null mutants bearing *sea-1*- and *sea-2*-null mutations (Fig. 3A). Forty-six percent of the *sea-3(y379); fox-1(y303) sex-1(y263)* XX triple mutants were viable compared with zero of the *fox-1 sex-1* mutants, and 42% of *sea-1(y356) sea-2(y426); sea-3(y379); fox-1(y303) sex-1(y424)* XX quintuple mutants were viable compared with 17% of the *sea-1(y356) sea-2(y426); fox-1(y303) sex-1(y424)* quadruple XX mutants (Fig. 3A). The fertility of the quintuple was also superior to that of the quadruple: Per adult, an average of 120 embryos were produced compared with 44 embryos, respectively.

In reciprocal experiments, all *sea-1(y356) sea-2(y426)* XO animals were viable, but 16% of the *sea-1(y356) sea-2(y426); sea-3(y379)* XO animals were inviable (Fig. 3C), showing that sufficient ASE function had been disrupted to block the full male-promoting activity of *xol-1*. The cumulative effect of *sea-1*, *sea-2*, and *sea-3* mutations in countering XSEs shows that ploidy, the autosomal component of the X:A signal, appears to be communicated by a set of discrete ASEs in a manner envisioned by Bridges for flies (Bridges 1921; see the Discussion).

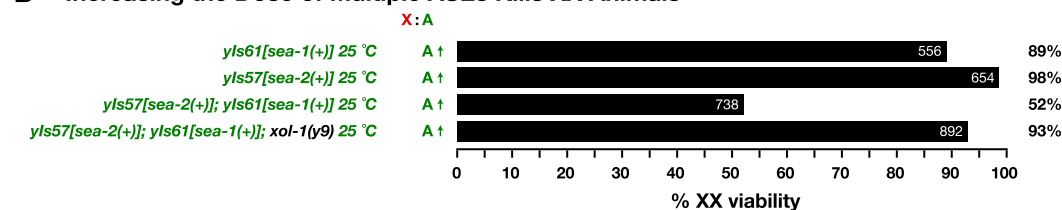
SEA-2 also controls sex determination and dosage compensation independently of *xol-1*

Precedent that an X:A signal element can control sex determination and dosage compensation by acting in two different capacities was set previously by *sex-1* (Gladden et al. 2007). SEX-1 functions as both an XSE to repress *xol-1* and an activator of hermaphrodite-promoting genes that function downstream from *xol-1* to activate dosage compensation (Supplemental Fig. S3A,B; Gladden et al. 2007). We asked whether *sea-2* also acts in two capacities. Our prior experiments showed that most, but not all, of the XX lethality caused by a *sex-1* mutation is suppressed by a *xol-1* mutation, and the residual lethality can be enhanced by RNAi against *sdcc-2*, a gene that acts downstream from *xol-1* to trigger assembly of the DCC onto X (Supplemental Fig. S3A). We show here that a *sea-2* mutation can partially suppress the residual XX lethality of *xol-1 sex-1* mutants (Supplemental Fig. S3B) and can partially suppress the enhanced XX lethality caused by *sdcc-2(RNAi)* of *xol-1 sex-1* mutants (Supplemental Fig. S3A). Moreover, increased dosage of *sea-2* assists *sdcc-2(RNAi)* in suppressing the XO lethality caused by a *xol-1* mutation (Supplemental Fig. S3C). Our combined results show that *sea-2* functions

A ASEs Act Cumulatively to Oppose XSEs



B Increasing the Dose of Multiple ASEs Kills XX Animals



C Reducing the Dose of Multiple ASEs Kills XO Animals

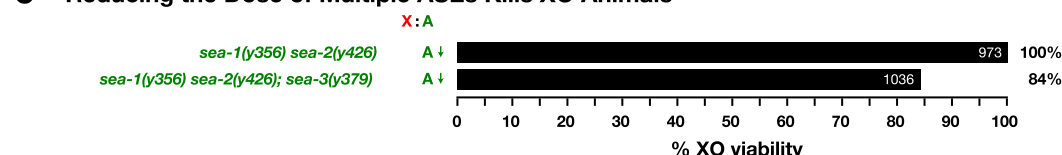


Figure 3. *sea-1*, *sea-2*, and *sea-3* act cumulatively to communicate ploidy. (A) Mutations in *sea-1*, *sea-2*, and *sea-3* together increase the viability of XSE-deficient XX animals more completely than knockout of only one or two ASEs. (B) Increased dosage of *sea-1* and *sea-2* more effectively reduces the viability of XX animals than increased dose of either alone. (C) Mutation of *sea-1*, *sea-2*, and *sea-3* together reduces XO viability. All strains carried the *him-8(e1489)* mutation, which increases the proportion of XO progeny to ~37%. Viability of XO animals bearing ASE mutations was determined by assessing the number of adult male progeny relative to those in the *him-8* control.

in two capacities to control the male modes of sex determination and dosage compensation: as an ASE to activate *xol-1* and as a repressor of a hermaphrodite-promoting activity that acts downstream from *xol-1*.

SEA-2 is an activator of *xol-1* transcription

XSEs communicate X-chromosome number by reducing the level of functional *xol-1* transcripts in a dose-dependent manner through two means: transcriptional repression and alternative mRNA splicing control. Because ASEs oppose XSEs, we asked whether SEA-2 communicates

the ploidy by increasing the level of functional *xol-1* transcripts. To assess the effect of SEA-2 on *xol-1* transcription, we used the integrated *yIs33* multicopy reporter transgene *Pxol-1::lacZ*, in which the *xol-1* promoter controls transcription of *lacZ* (Nicoll et al. 1997), to compare β -galactosidase activity among wild-type XX and XO embryos and XX embryos with increased *sea-2(+)* dose.

We first showed that the *xol-1* transcriptional reporter faithfully reproduces the activity states of *xol-1* in wild-type XX and XO embryos (Fig. 4A,B). Of embryos produced from *yIs33* XX animals, 90.1% had no detectable

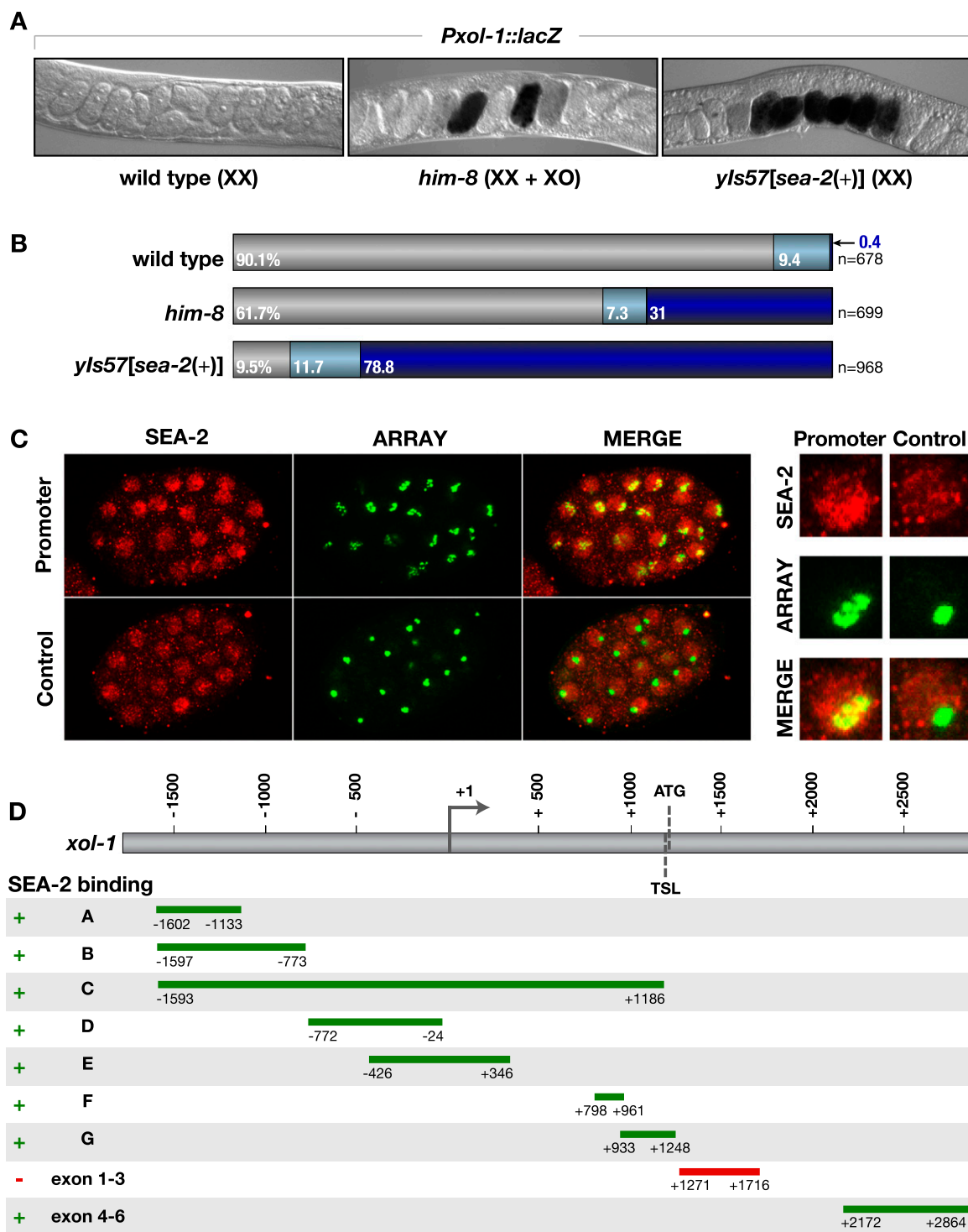


Figure 4. SEA-2 activates *xol-1* transcription by binding to the *xol-1* promoter. [A,B] Increased dose of *sea-2* activates transcription of *xol-1* in XX embryos. (A) Nomarski images of hermaphrodite gonads at 25°C from wild-type, *him-8*, and *yIs57[sea-2(+)]* transgenic animals carrying the integrated *Pxol-1::lacZ* transcriptional reporter. Hermaphrodites were grown at 25°C and stained for β -galactosidase activity. Embryos within the gonads have undetectable (light gray), low (gray), or high (black) levels of β -galactosidase activity. While wild-type and *yIs57[sea-2(+)]* hermaphrodites both produce only 0.2% XO embryos, *yIs57* hermaphrodites produce a higher frequency of embryos with high β -galactosidase activity, revealing that elevated *sea-2* dose activates *xol-1* in XX embryos. The level of β -galactosidase activity in *yIs57* XX embryos resembles that in XO embryos. The proportion of embryos with high and low β -galactosidase activity in *him-8* gonads reflects the expected proportion of XX to XO embryos. (B) Quantification of embryos having undetectable (gray), low (light blue), or high (dark blue) β -galactosidase activity within gonads of hermaphrodites with listed genotypes. *n* is the total number of embryos scored; percentages of embryos with each class of activity are indicated. (C) SEA-2 binds to *xol-1* in vivo. Confocal images of wild-type embryos bearing *xol-1* promoter arrays (fragment C in D) or control arrays both stained with SEA-2 (red) and GFP (green) antibodies. Arrays also contain a transgene encoding a GFP-tagged *lac* repressor protein (*lacI::GFP*) and multiple copies of *lac* operator sequences (*lacO*). *lacI::GFP* proteins bind to *lacO* sequences, allowing GFP antibodies to mark *xol-1* arrays. If endogenous SEA-2 protein binds to the *xol-1* promoter, SEA-2 antibodies colocalize (yellow) with GFP antibodies on arrays with *xol-1* but not control sequences. (D) Assessment of SEA-2-binding ability and map of assayed *xol-1* fragments in the promoter (1602 bp upstream of the TSS) and gene body (first 2864 bp). (+) SEA-2 binding to arrays, (–) no or rare binding to arrays.

β -galactosidase activity, and 0.4% had high activity. These results are consistent with the low level of *xol-1* activity in wild-type XX embryos, the low proportion (0.1%) of XO embryos in a wild-type brood, and the high level of *xol-1* activity in these rare XO embryos. Of embryos produced from *yIs33* XX animals bearing a *him-8* mutation, which elevates the proportion of XO progeny to 37%, 31% had high β -galactosidase activity, consistent with the increase in XO progeny. While the reporter transgene faithfully recapitulates *xol-1*'s sex-specific regulation, it does not reflect the absolute level of endogenous *xol-1* transcripts because the reporter is present in multiple copies, and its *lacZ* transcript level is higher than the endogenous *xol-1* transcript level. We next showed that increasing the dose of the wild-type *sea-2* gene increases *xol-1* transcription in XX animals (Fig. 4A). An array (*yIs57*) carrying multiple copies of *sea-2*(+) increased the proportion of *Pxol-1::lacZ*-bearing XX embryos having high β -galactosidase activity from 0.4% to 78.8%. These results indicate that SEA-2 activates *xol-1* transcription either directly or indirectly, and ASEs transmit ploidy by activating *xol-1* in a dose-dependent manner.

Identification of the *xol-1* transcription start site (TSS)

ASEs and XSEs antagonize each other to communicate the X:A signal by regulating *xol-1* transcription in opposite directions. To assess the mechanism by which these signal elements regulate *xol-1*, we first had to determine *xol-1*'s TSS. *xol-1*, like most genes in *C. elegans*, undergoes a cotranscriptional processing event in which the 5' end of the nascent transcript is replaced by a common 22-nt leader RNA through a *trans*-splicing mechanism. For *xol-1*, the *trans*-spliced leader (TSL) is spliced 14 nt upstream of the AUG start of translation (Rhind et al. 1995).

PCR amplification of *xol-1* cDNA made from embryo RNA revealed the TSS to be far upstream of the TSL site (Supplemental Fig. S5B). A robust PCR product placed the TSS at least 546 base pairs (bp) upstream of the TSL, and a faint product placed it further upstream, to at least 1037 bp. Because *trans*-splicing is cotranscriptional and TSSs are rarely identified accurately from accumulated RNA, we confirmed and extended our understanding of the *xol-1* TSS through our ongoing efforts to map genome-wide TSSs from nascent transcripts. Global run-on sequencing (GRO-seq) reactions were used to isolate nascent transcripts, and transcripts with 5' CAPs were then enriched and sequenced (WS Kruesi, LJ Core, CT Waters, JT Lis, and BJ Meyer, in prep.). The analysis confirmed our cDNA analysis and placed the *xol-1* TSS at 1203 nt upstream of the TSL, just downstream from a well-placed nucleosome (Supplemental Fig. S5A). In the early XX embryo, when *xol-1* is active prior to its repression by XSEs, this -1 nucleosome carries the H3K4me3 and H3K27ac post-translational modifications typical of active transcription (Supplemental Fig. S5C). Later in development, when *xol-1* is inactive, the modifications are absent.

The XSEs *SEX-1* and *CEH-39* repress *xol-1* transcription directly by binding to discrete sites in the promoter and gene body

To understand the basis for the molecular tug of war between XSEs and ASEs, we asked whether XSEs and ASEs bind directly to *xol-1* regulatory regions to control its transcription. Previous immunocytochemical experiments showed that SEX-1 colocalized in vivo with a *xol-1* promoter fragment that extends 1598 bp upstream of the TSS, drives sex-specific expression of a *Pxol-1::lacZ* transgene, and is responsive to *sex-1* mutations (Carmi et al. 1998). To detect SEX-1-binding sites within *xol-1*, we expressed and partially purified SEX-1 from Sf-9 insect cells and used SEX-1 in electrophoretic mobility shift assays (EMSAs) to survey 300-bp overlapping DNA probes spanning 1785 bp upstream of the TSS, the 1203-bp outtron, and the first three exons of *xol-1* (Fig. 5A; Supplemental Fig. S6A). Two sets of overlapping probes (J, K, and L, and P and Q) exhibited binding. The overlapping regions were further dissected by assaying SEX-1 binding to 50-bp overlapping probes. Five independent 25-bp SEX-1-binding regions were found: four in the promoter region overlapping the -1 nucleosome and one further along in the gene between the start points of transcription and translation. (Fig. 5A–C; Supplemental Figs. S5A, S6A,B).

The specificity in SEX-1 binding was established by antibody supershift experiments and mutational analysis. Increasing concentrations of SEX-1 antibody efficiently supershifted the already-shifted probes harboring the five candidate binding sites, demonstrating that SEX-1 was indeed bound to the probes (Fig. 5C; Supplemental Fig. S6B). Each of the five 25-bp binding regions encodes a close variant of the consensus nuclear hormone receptor (NHR)-binding site AGGTCA (Fig. 5C; Mangelsdorf et al. 1995). To validate these sequences as bona fide SEX-1-binding sites, we changed the first three bases of each candidate binding site to TTT and examined binding to the mutated sites (Fig. 5B). SEX-1 bound to none of the mutant probes. Our two findings that (1) SEX-1 binding was disrupted by mutation of the putative NHR response element and (2) the shift in wild-type probes was dependent on SEX-1 indicate that SEX-1 binds directly to *xol-1* regulatory sequences in vitro at five different sites. Of note, the closest two SEX-1 response elements are 48 bp apart, and no other NHR response elements reside nearby, suggesting that SEX-1 does not bind as a homodimer.

To identify CEH-39-binding sites, we performed EMSAs using CEH-39 produced from in vitro transcription-translation reactions and the 300-bp overlapping probes spanning the *xol-1* promoter and first three exons (Fig. 5D). CEH-39 bound to three sets of overlapping probes (H and I, K and L, and M and N) and two end probes (A and V) representing the promoter and third exon. Dissection of promoter region A revealed CEH-39 binding to two overlapping 50-bp probes that shared a version of the core ONECUT homeodomain consensus binding site ATTGAT (Fig. 5D,F; Supplemental Fig. S7) (Iyaguchi et al. 2007). CEH-39 binding was abrogated in subsequent EMSAs to site 1 by a mutation that changed the variant of the

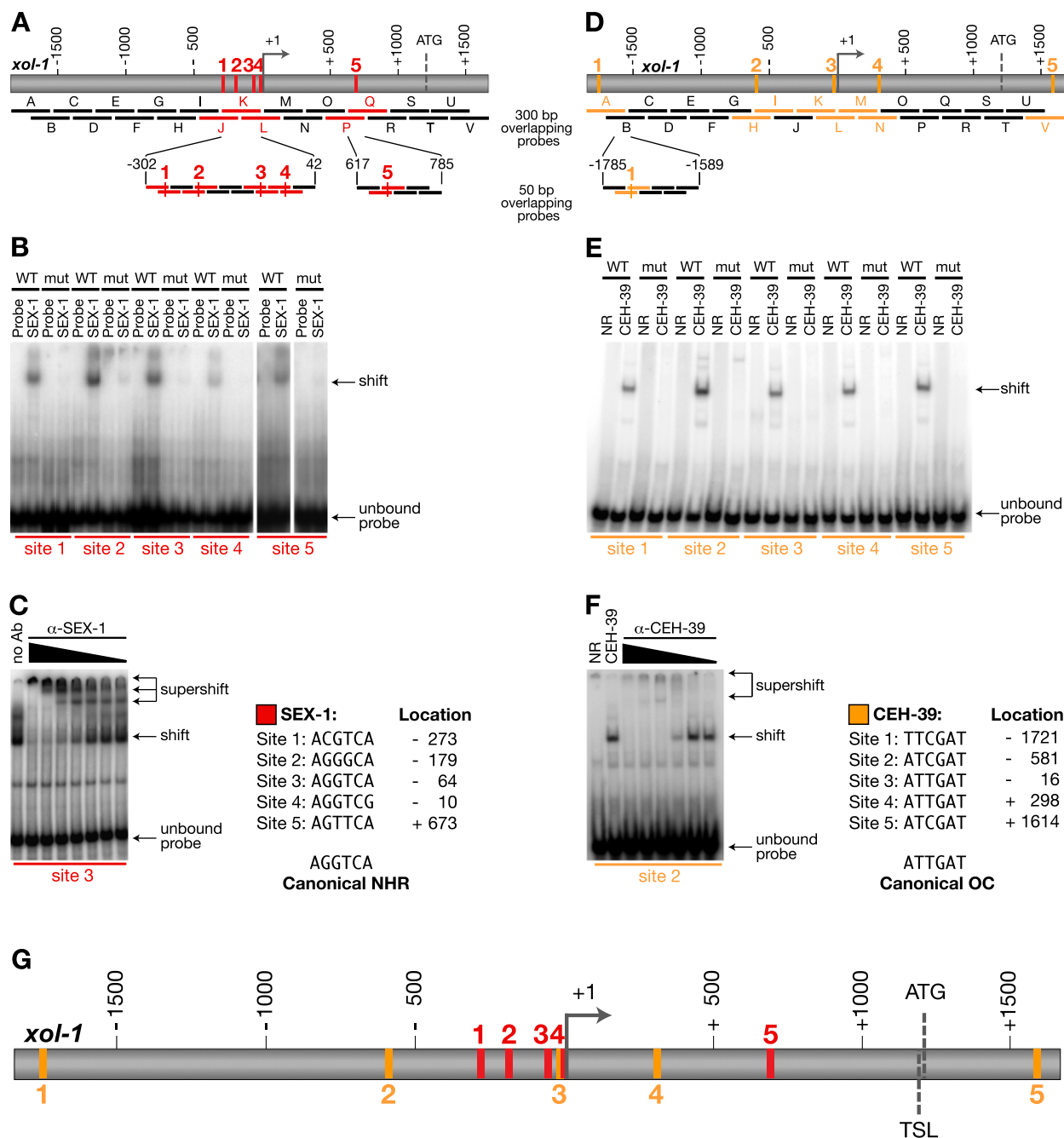


Figure 5. SEX-1 and CEH-39 bind directly to multiple discrete sites in *xol-1*. (A) Schematic diagram of the *xol-1* promoter and the 300-bp overlapping 32 P-labeled DNA fragments used for the SEX-1 EMSAs (A–V) shows the five SEX-1-binding regions (red). Positive probes were subdivided into 50-bp overlapping DNA fragments used to define the five discrete SEX-1-binding sites (red) using EMSAs. (B) Mutation of the nuclear hormone response elements eliminates SEX-1 binding to the 50-bp probes. Shown are SEX-1 EMSAs to either wild-type (WT) (right) or mutant (mut) (left) probes in which the first 3 bases of each SEX-1 response element was mutated to TTT. (C) Antibody supershift experiment for SEX-1-binding site 3. Increasing concentrations of SEX-1 antibody were titrated against a 50-bp probe incubated with a constant amount of SEX-1 extract. Supershifted bands (arrows) demonstrated the presence of SEX-1 in the original shifted protein–DNA complex. Sequences of the five SEX-1-binding sites are compared with a canonical NHR-binding site. Locations of sites are given relative to the TSS. (D) *xol-1* schematic for the 300-bp DNA fragments used in EMSAs with CEH-39 shows the location of CEH-39-binding regions (orange). Below is a schematic of 50-bp overlapping DNA fragments used to define the first CEH-39-binding site. (E) The homeodomain element in each CEH-39-binding site is required for CEH-39-dependent mobility shifts. Shown are EMSAs of either wild-type (WT) (right) or mutant (mut) (left) probes in which the homeodomain element within each binding site was mutated to GGGGGG. (F) Antibody supershift experiment for CEH-39-binding site 2. Increasing concentrations of CEH-39 antibody were titrated against the 50-bp probe that was incubated with a constant amount of CEH-39 protein. Supershifted bands (arrows) revealed the presence of CEH-39 in the original shifted band. Sequences and locations of CEH-39-binding sites are compared with a canonical ONECUT homeodomain-binding site. (G) Schematic of *xol-1* showing the SEX-1-binding site (red) and CEH-39-binding site (orange) relative to the TSS and the acceptor site for the SL1 TSL RNA.

consensus sequence to GGGGGG (Fig. 5E), thus demonstrating specificity in CEH-39 binding to classical ONECUT sites.

Similar ONECUT consensus sequences were found in each of the other CEH-39-bound probes (Fig. 5F). EMSAs demonstrated CEH-39 binding to unique 50-bp probes centered on each of the wild-type consensus sequences but not to probes carrying the GGGGGG mutated sequence (Fig. 5E). In total, we found three CEH-39-binding sites in the *xol-1* promoter: one between the start points of transcription and translation, and one in the third exon. One of the three promoter sites overlaps the -1 nucleosome (Supplemental Fig. S5A). Specificity of CEH-39 binding was further confirmed with antibody supershift experiments for all sites (Fig. 5F; data not shown).

Discovery of a CEH-39-binding site in the third exon helps explain our prior observation that the *yIs33* transcriptional *Pxol-1::lacZ* transgene reporter was responsive to *sex-1* mutations but not responsive to *ceh-39* mutations (Gladden and Meyer 2007). CEH-39 responsiveness required the reporter to contain the promoter and first three exons of *xol-1*.

One CEH-39-binding site (site 3) lies immediately adjacent to a SEX-1-binding site (site 4) with no nucleotides in between. Given the proximity of the sites, we tested whether CEH-39 and SEX-1 could bind as heterodimers and repress *xol-1* in a synergistic manner. No evidence was found for synergy between SEX-1 and CEH-39 binding to the same probe (data not shown). In aggregate, our experiments demonstrate that two XSEs—SEX-1 and CEH-39—bind directly to multiple sites throughout the *xol-1* regulatory region to control *xol-1*.

The ASEs activate xol-1 transcription directly by binding to discrete sites on the promoter and gene body

Although SEA-2 does not contain a well-defined DNA-binding domain, it does contain six separated zinc finger motifs, suggesting that SEA-2 might bind DNA. To assess SEA-2 binding to *xol-1*, we used the EMSA strategy outlined above using SEA-2 expressed from Sf-9 cells. We were unable to detect binding to any of the 300-bp probes. As an alternative approach, we assayed SEA-2 binding to *xol-1* in vivo using an immunocytochemical assay previously used to show colocalization of SEX-1 with the *xol-1* promoter (Fig. 4C,D; Carmi et al. 1998). We created transgenic strains carrying extrachromosomal arrays with multiple copies of either the *xol-1* promoter, *xol-1* promoter truncations, *xol-1* coding regions, or a control plasmid. These arrays also contained multiple copies of the *lac* operator (*lacO*) and a plasmid expressing a bifunctional lac repressor-GFP fusion protein (*lacI::GFP*). Colocalization of SEA-2 antibodies with *lacI::GFP* bound to *lacO* sites on the arrays implies SEA-2 binding to *xol-1*. SEA-2 colocalized with the full *xol-1* promoter, all of the promoter truncations, and exons 4–6 but failed to localize with the control and with exons 1–3 (Fig. 4C,D). These data show that SEA-2 associates with *xol-1* directly or indirectly via multiple sites throughout the gene.

In contrast to SEA-2, the ASE SEA-1 performed well in EMSA studies and enabled us to demonstrate that SEA-1 binds directly to the *xol-1* promoter (Fig. 6A–E; Supplemental Fig. S8). A SEA-1 fusion protein carrying an N-terminal GST tag was purified from bacteria and used in EMSA reactions with the 300-bp overlapping *xol-1* probes used for the XSE analysis. SEA-1 bound to two sets of overlapping probes (F and G, and R and S) and one individual probe (K). The regions of overlap and the unique K probe were dissected into small overlapping probes and analyzed with EMSAs (Fig. 6A; Supplemental Fig. S8). Four distinct SEA-1-binding sites were found throughout the *xol-1* promoter and one was found between the start points of transcription and translation. Two promoter sites overlap the -1 nucleosome (Supplemental Fig. S5A). The specificity of binding was confirmed by antibody supershift experiments (Fig. 6B; data not shown). The probes that bound SEA-1 do not harbor sequences resembling known T-box DNA-binding sites, except probes to binding site 1, which have limited similarity to the *Brachyury* half-site TTTCACACCT (Fig. 6E; Kispert and Herrmann 1993; Casey et al. 1998).

To identify the SEA-1-binding sites with greater precision, we performed DNase 1 footprinting assays with purified GST-SEA-1 on probes spanning the overlapping binding regions (Fig. 6D; Supplemental Fig. S9). Clear, distinct SEA-1 protected sites were found within each of the regions of overlap, all with unique sequences. Site 2 had the largest footprint. It had two shifted bands in EMSAs (Supplemental Fig. 8), suggesting that site 2 might have more than one SEA-1-binding site or that SEA-1 binds as a homodimer to this site and as a monomer to other sites. The importance of the identified sequences in SEA-1 binding was established through EMSAs with probes containing randomized sequences (Fig. 6C). SEA-1 binding was negligible to probes with randomized sequences but robust to the consensus T-box site used as a positive control.

SEA-1-binding sites are interspersed with SEX-1 and CEH-39 sites, but no clear overlap is evident between the ASE and XSE sites, implying that the antagonism between ASEs and XSEs is not simply due to direct competition for binding to overlapping sites (Fig. 6E). This interpretation is supported by the finding that the SEX-1 protein can supershift a SEA-1-bound DNA fragment carrying XSE- and ASE-binding sites, indicating that both elements can bind simultaneously to a single fragment of DNA (Supplemental Fig. 10).

Activation and repression of xol-1 transcription in vivo occurs via the XSE- and ASE-binding sites

To assess the importance of the XSE- and ASE-binding sites in vivo for the regulation of *xol-1*, we generated strains with integrated, single-copy *xol-1* transgenes bearing mutations in XSE- or ASE-binding sites and assayed their effect on hermaphrodite viability in wild-type and XSE- or ASE-deficient strains (Fig. 7A–C). The endogenous *xol-1* gene was knocked out in these strains, making the transgenes the sole source of *xol-1*. Three lines of evidence

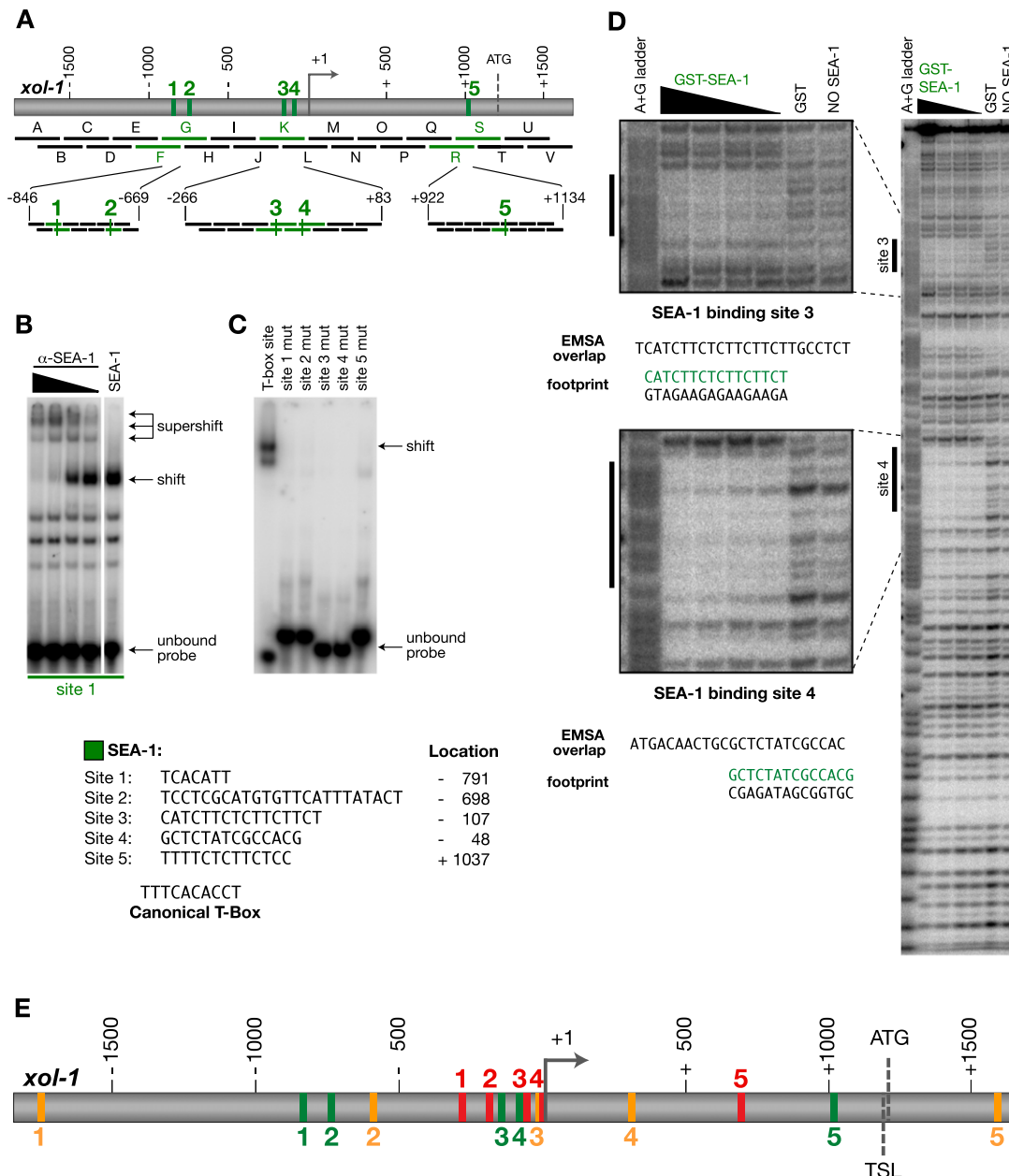





Figure 6. SEA-1 binds directly to multiple discrete sites in *xol-1*. (A) Schematic diagram of 300-bp *xol-1* DNA fragments used for EMSAs with SEA-1 shows the location of five SEA-1-binding regions (green). Below are the 30- or 50-bp overlapping fragments analyzed to define the five SEA-1-binding sites (green). (B) Antibody supershift experiment for SEA-1-binding site 1. Increasing concentrations of SEA-1 antibody were titrated against a 50-bp probe incubated with a constant amount of SEA-1 protein. Supershifted bands (arrows) revealed the presence of SEA-1 in the original shifted protein–DNA complex. (C) DNA sequences identified by the overlapping probes are required for the SEA-1-dependent mobility shifts. Shown are EMSAs with a probe of the consensus T-box site and probes carrying randomized versions of the five SEA-1-binding sites (mut). (D) DNase I footprinting assays identified five noncanonical T-box-binding sites for SEA-1. Shown is the 150-bp DNA fragment containing SEA-1-binding sites 3 and 4. The probe was incubated with either no protein, 600 ng of GST control, or a dilution series of 600, 300, 150, and 75 ng of GST-SEA-1. The protected regions (black bars) are enlarged at the left of the full-length gel. Each footprinting gel had a labeled A+G ladder as a marker for the protected sequences. Below each enlarged footprint are the sequences protected by SEA-1 compared with the overlapping sequence in the probes bound by SEA-1 in EMSAs. The radiolabeled and interrogated DNA strand is shown in black, and the reverse strand in green matches the site shown in E. The five SEA-1-binding sites identified by footprinting assays are compared with a canonical T-box-binding site. (E) Schematic of *xol-1* with the SEA-1-binding site (green), SEX-1-binding site (red), and CEH-39-binding site (orange).



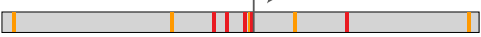
showed that mutating the XSE- and ASE-binding sites in *xol-1* recapitulated the phenotypes caused by disrupting the XSE and ASE genes. First, disrupting all SEX-1- and

CEH-39-binding sites in a *xol-1* transgene killed nearly all *xol-1* transgenic XX mutant animals, just as disrupting both *ceh-39* and *sex-1* killed all XX animals (Fig. 7A). The

A Mutation of ASEs suppresses the ♀ lethality due to deletion of XSE binding sites in a *xol-1* transgene

	♀ Viability
 <i>xol-1(+) transgene</i> in <i>xol-1</i> mutant background	94% (820)
 <i>xol-1 transgene with ΔSEX-1 and ΔCEH-39 sites</i> in <i>xol-1</i> mutant background	0% (dead)
 <i>xol-1 transgene with ΔSEX-1 and ΔCEH-39 sites</i> in <i>sea-1 sea-2; xol-1</i> mutant background	93% (728)

B Deletion of SEA-1 binding sites in a *xol-1* transgene suppresses the ♀ lethality of *sex-1* null mutants

 <i>xol-1(+) transgene</i> in <i>xol-1</i> mutant background	94% (528)
 <i>xol-1(+) transgene</i> in <i>xol-1 sex-1</i> mutant background	18% (122)
 <i>xol-1 transgene with ΔSEA-1 sites</i> in <i>xol-1 sex-1</i> mutant background	38% (210)

C The *xol-1* transgene lacking SEA-1 binding sites suppresses the ♀ lethality due to XSE mutations


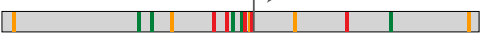
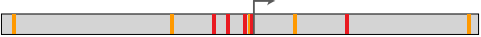
 <i>xol-1(+) transgene</i> in <i>xol-1</i> mutant background	95% (782)
 <i>xol-1(+) transgene</i> in <i>fox-1 xol-1 sex-1</i> mutant background	0% (412)
 <i>xol-1 transgene with ΔSEA-1 sites</i> in <i>fox-1 xol-1 sex-1</i> mutant background	12% (930)

Figure 7. Mutation of XSE- and ASE-binding sites in *xol-1* transgenes, the sole source of *xol-1* in the strains, recapitulates the phenotypes caused by disrupting the XSE and ASE genes. Single-copy, integrated *xol-1* transgenes bearing mutations in either XSE- or ASE-binding sites were assayed for their effect on hermaphrodite viability in different mutant backgrounds. Descriptions of *xol-1* transgenes and genotypes of assayed XX animals are indicated *below* each schematic of the regulatory region. Viability is shown to the *right*, with the number of embryos counted (*n*) in parentheses. Hermaphrodite viability was calculated from at least three independent experiments using the formula [(no. of adult hermaphrodites)/(total no. of embryos)] × 100. (A) Disruption of the ASE genes *sea-1* and *sea-2* in XX animals carrying a *xol-1* transgene lacking binding sites for the XSEs SEX-1 and CEH-39 restored XX viability to nearly wild-type levels. In the control strain bearing mutations in *sea-1* and *sea-2*, 98% of animals were viable (*n* = 723). The genotype was *sea-1(y356) sea-2(y407); xol-1(y9); yIs[xol-1]*. (B) Disruption of SEA-1-binding sites in a *xol-1* transgene partially suppressed the XX lethality of *sex-1*(null) XX mutants. (C) Disruption of SEA-1-binding sites in a *xol-1* transgene partially suppressed the XX lethality of *fox-1 sex-1* XX mutants. In the control strain carrying a *xol-1* transgene with disrupted SEA-1-binding sites, 93% of animals were viable (*n* = 653).

hermaphrodite lethality caused by disrupting XSE-binding sites in the transgene was fully suppressed by disrupting both the *sea-1* and *sea-2* genes (Fig. 7A).

Analysis of *xol-1* transcript levels from wild-type and XSE-binding-defective transgenes further corroborated the function of the XSE-binding sites *in vivo* (Supplemental Table S1). *xol-1* transcript levels from a wild-type transgene were elevated 3.5-fold in a *sex-1(y424)*-null mutant compared with a *sex-1(+)* mutant, in close agreement with the 2.8-fold increase in *xol-1* transcript level from the endogenous gene in a *sex-1(y424)* mutant. Furthermore, *xol-1* transcript levels from a *xol-1* transgene with mutations

in all SEX-1- and CEH-39-binding sites were increased further, to 6.9-fold, consistent with the mutations eliminating the repressive function of XSEs.

Second, just as a *sea-1* mutation prevented the death of many *sex-1* XX mutants (Fig. 3A), knocking out the SEA-1-binding sites in the *xol-1* transgene prevented the death of many *sex-1* XX mutants that would be caused by a wild-type *xol-1* transgene (Fig. 7B). Third, just as a *sea-1* mutation prevented the death of many *fox-1 sex-1* double mutants (Powell et al. 2005), knocking out the SEA-1-binding sites in the *xol-1* transgene prevented the death of many *fox-1 sex-1* XX mutants that would be caused by

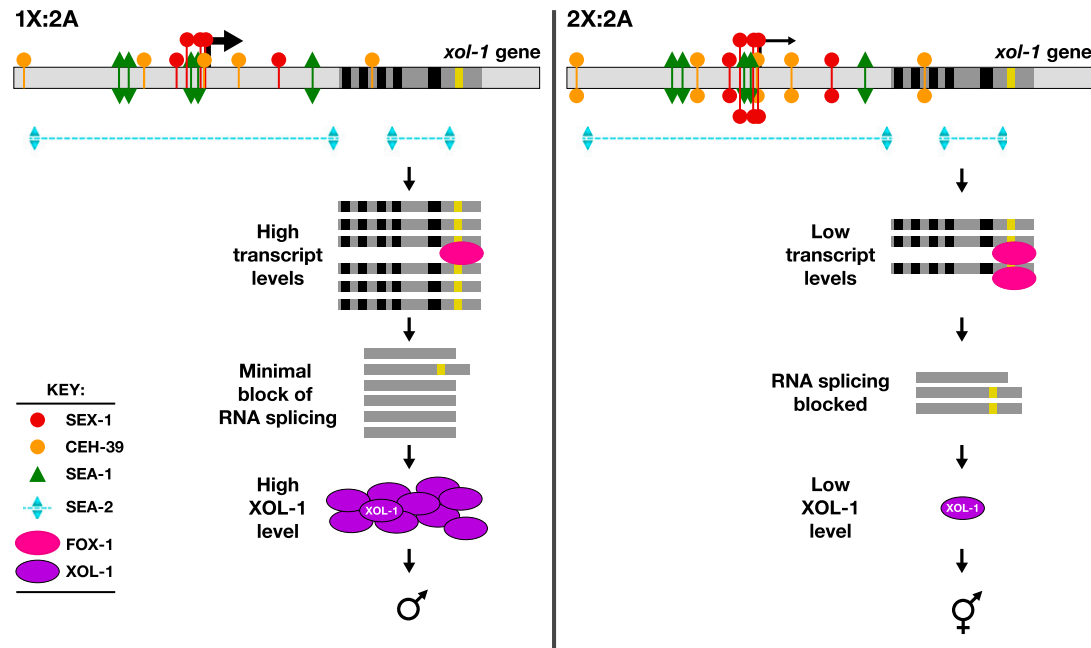


Figure 8. Primary sex determination: model for X:A signal assessment. XSEs and ASEs bind directly to numerous sites on *xol-1* and antagonize each other to control *xol-1* transcription and thereby determine *C. elegans* sex. Molecular rivalry at the *xol-1* promoter between XSE transcriptional repressors (the ONECUT homeodomain protein CEH-39 and the NHR SEX-1) and ASE transcriptional activators (the T-box transcription factor SEA-1 and the zinc finger protein SEA-2) leads to high *xol-1* transcript levels in XO embryos with one dose of XSEs and low levels in XX embryos with two doses of XSEs. The RNA-binding protein FOX-1, an XSE, then enhances the fidelity of the counting process in by blocking proper RNA splicing of the sixth intron (yellow) in a dose-dependent manner, resulting in *xol-1* mRNA splice variants with in-frame stop codons. High XOL-1 protein levels in XO animals induce male development, and low XOL-1 levels in XX animals induce hermaphrodite development, including loading of the DCC onto X.

a wild-type *xol-1* transgene (Fig. 7C). These results show that the XSE- and ASE-binding sites identified by in vitro binding studies are critical for the regulation of *xol-1* in vivo. Thus, XSEs and ASEs oppose each other to transmit the X:A signal by regulating *xol-1* transcription directly but in opposite ways.

Discussion

Sex is determined in many organisms by a chromosome-counting mechanism that distinguishes one X chromosome from two. Here we dissected one such precise counting mechanism in molecular detail to understand how small changes in the concentrations of molecular signals can be translated into different developmental fates. Rather than counting the absolute number of X chromosomes, the nematode *C. elegans* assesses the number of X chromosomes relative to the sets of autosomes. We showed previously that a set of genes on X, called XSEs, communicates the embryo's X-chromosome dose by repressing the activity of the master sex-determining gene *xol-1* in a cumulative, dose-dependent manner. *xol-1* is active and induces the male fate in embryos with one dose of XSEs (1X:2A) but is repressed in embryos with two doses of XSEs (2X:2A), permitting the hermaphrodite fate. Here we identified elements of the autosomal signal and showed that the dose of autosomes is communicated by a corresponding set of ASEs that act in a

cumulative, dose-dependent manner to counter XSEs by stimulating *xol-1* transcription. We further showed that XSEs and ASEs bind directly to the 5' regulatory region of *xol-1* to antagonize each other's activities and thereby set the level of *xol-1* transcription to reflect the X:A sex determination signal (Fig. 8). Hence, multiple antagonistic molecular interactions carried out on a single promoter form the basis of the primary sex determination decision in *C. elegans* and make the sex determination process highly responsive to the relative dose of X chromosomes and autosomes (Fig. 8).

Of the XSEs, the NHR SEX-1 and the ONECUT homeodomain protein CEH-39 bind directly to five non-overlapping *cis*-acting regulatory sites on the *xol-1* promoter and gene body to repress transcription. SEX-1-binding sites resemble canonical NHR sites, and CEH-39-binding sites resemble canonical ONECUT homeodomain sites. Disrupting all SEX-1 and CEH-39 sites on a *xol-1* transgene in vivo recapitulated the derepression of *xol-1* and consequent XX lethality caused by disrupting the respective XSE genes. This XX lethality was rescued by mutations in the ASEs *sea-1*, which encodes a T-box transcription factor, and *sea-2*, which encodes a zinc finger protein, establishing that SEX-1 and CEH-39 repress *xol-1* directly by binding to it.

SEA-1 also binds directly to five sites on the *xol-1* promoter and gene body. While SEA-1 can bind to canonical T-box sites in vitro, the *xol-1* sites are variable in

length and do not resemble canonical T-box-binding sites, suggesting that it belongs to a different class of T-box transcription factors. Disrupting the SEA-1-binding sites on a *xol-1* transgene also reiterated the effects of knocking out the endogenous *sea-1* gene. The binding site mutations partially suppressed the XX lethality caused by a *sex-1*-null mutation or the *fox-1 sex-1* double-mutant combination, confirming that SEA-1 binds directly to *xol-1* to stimulate its transcription. While the purified SEA-2 protein failed to bind *xol-1* DNA in vitro, SEA-2 did bind in vivo to multiple sites on the *xol-1* promoter and gene body, indicating that SEA-2 activates *xol-1* transcription directly.

The autosomal signal also includes the ASE *sea-3*, which collaborates with *sea-1* and *sea-2* to oppose XSEs and thereby promote the male fate. Its molecular cloning has not yet been achieved. Disrupting all three *sea* genes suppresses the XX lethality caused by loss of XSEs significantly more than just disrupting *sea-1* and *sea-2*. Furthermore, disrupting all three *sea* genes reduced the autosomal signal sufficiently to kill males due to inadequate activation of *xol-1*. Hence, these three elements function together as strong *xol-1* activators. Nevertheless, the fact that some triple-mutant XO animals survive reveals that additional ASEs must contribute to the autosomal signal. Our screen likely failed to identify other ASEs because *Mos1* has a 30% average transposition frequency (Williams et al. 2005), and only 9400 mutagenized haploid genomes were screened.

A prior study demonstrated that *sex-1* promotes the hermaphrodite fate by acting in two capacities: as an XSE to repress *xol-1* and as an activator of hermaphrodite-promoting genes that function downstream from *xol-1* to activate dosage compensation (Gladden et al. 2007). *sex-1* exerts the majority of its sex-determining function through *xol-1*. Similarly, our study demonstrated that *sea-1* and *sea-2* function in two capacities to control the male modes of sex determination and dosage compensation: as an ASE to activate *xol-1* and as a repressor of hermaphrodite-promoting activity that acts downstream from *xol-1*. Like *sex-1*, both *sea-1* and *sea-2* exert the majority of their sex-determining function by acting on *xol-1*. We note, though, that *sea-2* has roles in development beyond controlling sex determination and dosage compensation. Huang et al. (2011) demonstrated a role for *sea-2* in regulating larval developmental timing and adult life span.

The worm X:A-counting mechanism fits Bridges' 1921 textbook paradigm for fly sex determination, but the fly mechanism does not

While our study shows that the worm X:A-sensing process fulfills Bridges' proposed model for fly sex determination involving a set of feminizing genes on X and an antagonistic set of masculinizing genes on autosomes (Fig. 8; Bridges 1921), others have shown recently that the fly X:A-sensing process does not (Barbash and Cline 1995; Erickson and Quintero 2007). In the fruit fly, the target of the X:A signal is *Sxl* (sex-lethal), a sex-determining switch gene that induces female development when

active and male development when inactive (Cline and Meyer 1996). A set of feminizing XSEs communicates X-chromosome number (Cline 1988; Erickson and Cline 1991, 1993; Sefton et al. 2000) by activating *Sxl* transcription in a dose-dependent manner. The double dose of XSEs in 2X:2A embryos turns *Sxl* on, while the single dose in 1X:2A embryos does not. In contrast, ploidy appears not to be signaled by a corresponding set of masculinizing autosomal genes (Barbash and Cline 1995; Erickson and Quintero 2007). Instead, the effect of ploidy in this dose-sensitive process is indirect, influencing the timing of cellularization during early development and thereby the length of time during which XSE protein can increase in concentration to reach the threshold necessary to activate *Sxl* (Erickson and Quintero 2007). The lower the ploidy, the later the embryos cellularize, the longer the XSEs can accumulate, and the higher the probability of activating *Sxl*. As a consequence, 1X:1A embryos become females instead of males, and 2X:3A embryos become mosaic intersexes. Only a single fly ASE was identified through extensive genetic screens to identify suppressors of XSE mutations (Barbash and Cline 1995). That ASE acts as a weak transcriptional repressor of *Sxl* and is thought to function relatively late to fine-tune the counting process in diploids.

Models for antagonistic molecular interactions between worm XSEs and ASEs

Given the numerous binding sites for XSEs and ASEs on the *xol-1* gene, how do these signal elements counteract each other to promote opposite transcriptional states? The findings that XSE- and ASE-binding sites are distinct and nonoverlapping and that SEX-1 and SEA-1 can bind simultaneously to the same DNA fragment suggest that direct competition for binding to *xol-1* is not likely to underlie the antagonistic molecular interactions between these XSEs and ASEs at the *xol-1* promoter. Instead, because nuclear receptors, ONECUT homeobox proteins, and T-box proteins repress or activate transcription by tethering corepressors or coactivators to their gene targets (Asahara et al. 1999; Maira et al. 2003; Privalsky 2004; Murakami et al. 2005), an attractive alternative model is that XSEs and ASEs recruit cofactors with reciprocal enzymatic activities to the *xol-1* promoter to elicit opposite transcriptional states. Common cofactors are those that modify histones to regulate transcription, including histone acetyltransferases and methyltransferases for gene activation and histone deacetylases for gene repression (Privalsky 2004; Lee et al. 2005a,b).

Our identification here of the true *xol-1* TSS revealed that the 5' region with the highest density of SEX-1-, CEH-39-, and SEA-1-binding sites overlaps the –1 nucleosome, which carries post-translational modifications positively correlated with *xol-1* activity (Supplemental Fig. S5A–C). In young embryos, when *xol-1* is active prior to its repression by XSEs, the nucleosome carries the H3K4me3 and H3K27ac modifications typical of transcribed genes. Nucleosomes in the gene body also carry modifications typical of transcription elongation: H3K79me3 and

H3K36me3. All four modifications are absent later in development, when *xol-1* is repressed. Regulation of the post-translational modification of the -1 nucleosome by ASEs and XSEs is a highly plausible mechanism for at least part of the antagonism between XSEs and ASEs.

T-box proteins can trigger the acetylation of histones and achieve transcriptional activation during development. For example, the T-box transcription factor TBX5 plays an essential, dose-dependent role in both cardiac and limb development (Mori and Bruneau 2004; Murakami et al. 2005). As with *sea-1*, the *TBX5* gene is haploinsufficient. Patients with Hold-Oram syndrome carry heterozygous mutations in *TBX5* and have defects in their heart and upper extremities. TBX5 recruits the coactivator TAZ to stimulate transcription of TBX5-dependent promoters by tethering the histone acetyltransferase proteins p300 and PCAF to the TBX5-binding sites. Similarly, NHRs such as SEX-1 are known to tether histone deacetylases and histone demethylases to their binding sites through corepressors to repress transcription (Privalsky 2004; Rosenfeld et al. 2006; Cai et al. 2011).

In our model, ASEs such as SEA-1 and SEA-2 would accumulate in high concentration at the *xol-1* promoter of young embryos to activate transcription in part by catalyzing the acetylation of the -1 nucleosome. In embryos with a double dose of XSEs, sufficient XSE protein would accumulate on the *xol-1* promoter over time to repress transcription in part by catalyzing the deacetylation of the -1 nucleosome and perhaps the demethylation of nucleosomes in the gene body. This type of molecular antagonism requires that ASEs and XSEs accumulate on the *xol-1* promoter at overlapping times, when the X:A signal is being assessed. Two lines of evidence support this condition. Both SEA-1 and SEX-1 can bind together in vitro to a single fragment of *xol-1* DNA that encodes the highest density of XSE- and ASE-binding sites. Also, SEX-1 and SEA-2 colocalize with *xol-1* regulatory regions in vivo at overlapping times, from at least the 20-cell stage when *xol-1* is active until after the 60-cell stage, when *xol-1* expression becomes significantly repressed.

The competing mechanisms of *xol-1* activation and repression need not be limited to the regulation of histone modification at the TSS. In general, corepressors recruited by NHRs and ONECUT homeodomain proteins can make inhibitory contacts directly with the basal transcription machinery to limit transcription (Baniahmad et al. 1993; Muscat et al. 1998; Wong and Privalsky 1998), and co-activators recruited by T-box proteins can make productive contacts with the basal machinery to stimulate transcription (Kwok et al. 1994; Yao et al. 1996; Maira et al. 2003). The locations of ASE- and XSE-binding sites throughout the promoter and first part of the gene are well positioned to permit such direct inhibitory and stimulatory contacts with the transcription machinery.

Synergy in XSE action

The high degree of specificity for SEX-1 and CEH-39 in sex determination cannot be explained completely by the 6-bp response elements within the XSE-binding sites. The

elements by themselves are too short to confer strong stability in XSE binding to *xol-1*. Binding is likely enhanced through the association of XSEs with each other or with other more general DNA-binding proteins. Given that XSEs function cumulatively and mutations in *sex-1* and *ceh-39* act synergistically, the possibility existed that SEX-1 and CEH-39 might bind to *xol-1* cooperatively, and the cooperativity might help the stability and specificity. However, in vitro binding studies of SEX-1 and CEH-39 to probes with neighboring NHR- and ONECUT-binding sites failed to demonstrate cooperative binding in gel shift assays (data not shown).

NHRs and homeodomain proteins commonly bind target genes as homodimers or as heterodimers with proteins of their respective class via closely spaced response elements (Mangelsdorf et al. 1995). Dimerization enhances the stability and specificity in binding. However, the two closest SEX-1 response elements are 48 bp apart with no NHR recognition elements nearby, and the closest CEH-39 response elements are 308 bp apart, suggesting that SEX-1 and CEH-39 bind *xol-1* as monomers. SEX-1 and CEH-39 are thus likely to associate with other unidentified transcription factors or with corepressors tethered to other DNA-binding proteins that confer increased binding stability by contributing additional contacts with DNA. The synergy between SEX-1 and CEH-39 in repressing *xol-1* transcription would then derive from the aggregate effect of XSEs making multiple independent contacts with *xol-1* regulatory sequences to elicit inhibitory contacts with the basal transcription machinery through corepressors and/or to recruit corepressors with the same or different enzymatic activities to repress transcription in part by altering nucleosome post-translational modification. To date, only a single NHR corepressor molecule (DIN-1) has been identified functionally in *C. elegans* (Ludewig et al. 2004), and we found that it does not function in the sex determination pathway (data not shown).

Although transcriptional repression is the predominant form of *xol-1* regulation by XSEs, they also repress *xol-1* through a post-transcriptional mechanism. The XSE FOX-1 binds the sixth intron of *xol-1* pre-mRNA and thereby blocks productive *xol-1* mRNA splicing, generating an in-frame stop codon (C Pickle, M Nicole, and BJ Meyer, in prep.). This splicing control enhances the fidelity of the counting process once the transcriptional regulation has occurred (Fig. 8). *fox-1* mutations cause no XX-specific lethality by themselves but cause synergistic lethality in combination with *sex-1* mutations.

Another influence on the target of the X:A signal?

A negative regulatory feedback loop has been proposed to repress *xol-1* by the terminal feminizing switch gene in the sex determination regulatory hierarchy *tra-1* (Hargitai et al. 2009). The TRA-1 zinc finger protein represses male differentiation genes and induces hermaphrodite differentiation genes. The loop is proposed to function after X:A assessment, perhaps to maintain a low *xol-1* activity state in XX embryos once the major sex determination decision has been made and sexual differentiation is

under way. Partial loss of *tra-1* was reported to cause significant XX lethality that could be suppressed by mutations in *xol-1*. A TRA-1-binding site was found in *xol-1* at +1045 with respect to our new TSS. We investigated the contribution of *tra-1* to the repression of *xol-1* and found the contribution to be minimal compared with that reported by Hargitai et al. (2009) (Supplemental Fig. 11). We found that complete loss of *tra-1* caused very little XX lethality under standard growth conditions, and none of the lethality was suppressible by a *xol-1*-null mutation, indicating that misregulation of *xol-1* was not the cause of lethality. We did find some *xol-1*-suppressible lethality under more extreme growth conditions but less than reported previously, and the escapers had no dosage compensation defects, unlike XSE mutants. Hence, a repressive interaction between *tra-1* and *xol-1* is unlikely to constitute a significant feedback loop.

Implications of the X:A signal for development and disease

The classes of regulatory molecules that play critical roles in the X:A-sensing process—NHRs, ONECUT homeodomain proteins, and T-box proteins—also have central roles in development, homeostasis, and reproduction, even in humans. For all of these functions, the dose sensitivity of genes encoding the regulatory molecules underlies the pathologies and developmental disorders. As examples, haploinsufficiency of the nuclear receptor steroidogenic factor (SF-1) causes XY sex reversal and adrenal failure in humans (Achermann et al. 1999; Bland et al. 2000); haploinsufficiency of the T-box gene *TBX1* causes DiGeorge syndrome, characterized by cardiovascular, thymus, and craniofacial anomalies (Lindsay et al. 2001; Baldini 2006); and haploinsufficiency of the homeobox gene *Pitx2* causes Rieger syndrome type 1, characterized by ocular, dental, abdominal, and craniofacial malformation (Flomen et al. 1998; Liu et al. 2003). The underlying molecular defects triggered from inappropriate gene dose are not known for these human diseases, but advances in our molecular understanding of the X:A-sensing process in *C. elegans* provide a guide for future investigations.

Materials and methods

Isolation of *sea-2* alleles

For each ASE screen, the final mutagenesis strain *fox-1 sex-1; yEx660; oxEx229* was created by crosses using two initial strains (see Fig. 1B): (1) a *fox-1 sex-1* XX strain carrying the transgenic extrachromosomal array *yEx660* [*dpy-30::sdc-2(+)*] (30 ng/ μ L), *hsp-16-48::Mos1* transposase (10 ng/mL), *unc-122::gfp* (30 ng/mL), and genomic DNA (200 ng/ μ L)] and (2) a strain carrying *oxEx229* (*Mos1, myo-2::gfp*) (Bessereau et al. 2001). All crosses were performed at 25°C to prevent germline silencing of the arrays. Approximately 50 double-transgenic animals were subjected to heat shock per screen as follows: 1 h at 33°C, 1 h of recovery at 15°C, 1 h at 33°C, and 20 h of recovery at 15°C. F1 progeny were examined by PCR to determine *Mos1* transposition frequency per screen (30%–40%). We obtained 619 viable nongreen hermaphrodites from F2 progeny representing 9400

Mos1 mutagenized haploid genomes. Only 120 of 619 produced viable F3 progeny, and only 30 of 120 contained the *Mos1* transposon. *Mos1*-containing strains were outcrossed at least four times, and only five of 30 strains had the transposon linked to the suppression phenotype. The transposon insertion site was identified in each strain by inverse PCR as described in Bessereau et al. (2001). For each insertion allele, the corresponding ORF was disrupted by RNAi in a *fox-1 sex-1* double mutant. RNAi of only K10G6.3 phenocopied the suppression of *fox-1 sex-1* lethality to the same degree as the corresponding insertion allele. This screen yielded *sea-2(y407)*, which has a *Mos1* insert in exon 4 but is not a null allele. A *sea-2*-null allele was obtained by excising the *Mos1* transposon from *sea-2(y407)*, and *sea-2(y410)* was isolated from a deletion library (see the Supplemental Material).

Genetic analysis and phenotypic characterization

Hermaphrodite viability was assessed by picking one to three L4 larvae per plate, serially transferring animals every 24 h for 2–3 d, counting the number of embryos and L1s after transfer, and counting the total adults 4–5 d after plating the original L4s. Percent viability was calculated as [(total number of adults)/(total number of embryos)] \times 100.

The effects of changing *sea-2* activity on the viability of males with an extra copy of both *ceh-39* and *fox-1* (on *yDp14 X:I*) was assessed by either crosses or analysis of strains carrying *him-8(e1489)*. (1) To assess the viability of *yDp14/+* males (Fig. 2C), wild-type males were crossed with *yDp14 X:I; rol-6(e187 II); unc-2(e55) X*, and the non-Rol cross progeny (*yDp14/+; rol-6/+; unc-2/+ XX* or *yDp14/+; rol-6/+; unc-2 XO*) animals were counted. Percent male viability was calculated by the formula [(total number of males observed)/(total number of males expected)] \times 100, where the expected male frequency is equal to the number of hermaphrodite cross progeny observed. (2) To assess the viability of *sea-2(y426)/+; yDp14/+* males (Fig. 2C), *sea-2(y426)* males were crossed with *yDp14 X:I; rol-6(e187 II); unc-2(e55) X* hermaphrodites, and progeny were analyzed as above. Surviving heterozygous male cross progeny [*yDp14/+; sea-2(y426)/rol-6(e187); unc-2(e55)*] were crossed back to *yDp14; rol-6(e187); unc-2(e55)* hermaphrodites to create homozygous *yDp14; sea-2(y426); unc-2* hermaphrodites. (3) To assess the viability of *sea-2(y426)/sea-2(y426); yDp14/+* males (Fig. 2C), *sea-2(y426)* males were crossed with *yDp14; sea-2(y426); unc-2* hermaphrodites, and cross progeny were analyzed as above. (4) To assess the viability of *yDp14/+; sea-2(y407)/+* males and *yDp14/+; yIs57 [sea-2(+)]* males (Fig. 2E), progeny from the *him-8(e1489)* strains were analyzed as follows. For *yDp14/+* male viability, the relative number of *yDp14/+; him-8(e1489); unc-2(e55)* (non-Unc) and *+/+; him-8(e1489); unc-2(e55)* (Unc) male self-progeny were counted from *yDp14/+; him-8(e1489); unc-2(e55)* hermaphrodites. Of the male progeny, one-fourth are expected to be Unc; one-fourth are expected to die (*yDp14* homozygotes), and one-half are expected to be non-Unc. Percent male viability was calculated as [(total number of non-Unc males observed)/(total number of non-Unc males expected)] \times 100, where the number of expected males is equal to two times the number of Unc males observed. Self-progeny from *yDp14/+; sea-2(y407); him-8(e1489); unc-2(e55)*, and *yDp14/+; yIs57 him-8(e1489); unc-2(e55)* hermaphrodites were counted as above. *yDp14/+* male viability is typically higher in the progeny of homozygous *him-8(1489)* hermaphrodites than in the progeny from crosses.

SEA-2 antibody

Rabbit anti-SEA-2 antibodies were raised and affinity-purified against a C-terminal 21-amino-acid peptide (CG-linker)RMA

DQFMMNTNYTTPPTHVQL. Embryos were fixed and stained as described (Powell et al. 2005).

xol-1 reporter assay

The integrated transgenic reporter *yIs33(Pxol-1::lacZ)* used to assess β -galactosidase activity in XO, XX, and *sea-2*-overexpressing (*yIs57*) embryos at 20°C or 25°C contains 1633 bp of *xol-1* regulatory sequences upstream of the TSS and 1203 bp between the TSS and the TSL site, which was fused to the *lacZ* ORF and 3' *unc-54* untranslated region (UTR) (Nicoll et al. 1997). Worms were grown for two generations at each temperature, and gravid adults were fixed and stained as described (Fire 1992). Embryo staining was examined using differential interference contrast (DIC) microscopy, and >600 embryos were examined from >50 hermaphrodites for each genotype. Embryos were classified as having no (or weak), moderate, or high staining.

Protein expression and purification

SEX-1 was expressed in Sf-9 cells using the Bac-to-Bac Baculovirus Expression system (Invitrogen) and nuclear extracts prepared as described (Chen et al. 1993), with the exception that the hypertonic buffer was supplemented with 0.8 mM KCl and 1% NP-40. For control nuclear extracts, nonrecombinant baculovirus was used to infect Sf-9 cells, and nuclear extracts were prepared as above. Protein expression was examined by SDS-PAGE/Western blotting and Coomassie staining, and protein concentrations were determined by Bradford assay (Thermo Scientific).

Full-length SEA-1 encoding cDNA was cloned into pGEX-4T (GE Biosciences) as an N-terminal GST fusion expression construct and expressed in BL21 cells (Smith and Johnson 1988). Cells were induced with IPTG for 2 h at 37°C, and protein was extracted. Cells were resuspended in STE buffer (150 mM NaCl, 10 mM Tris at pH 8.0, 1 mM EDTA) supplemented with 100 μ g/mL lysozyme, 3 mM DTT, 1.5 mM PMSF, and 1% Triton X-100, incubated on ice for 20 min, frozen in liquid nitrogen, and thawed immediately at room temperature. The homogenate was then supplemented with 0.8 M NaCl, 0.5% NP-40, and 5 mM DTT and sonicated. Cleared supernatant was then incubated with glutathione agarose in STE buffer and washed in a stepwise fashion in STE buffer supplemented with 500 mM NaCl and STE buffer supplemented with 250 mM NaCl, and bound protein were eluted. GST was purified in an identical manner using the empty pGEX-4T3 vector. All steps of the purifications were assessed on a 10% acrylamide gel (37.5:1) by Coomassie staining, and protein concentrations were determined by Bradford assay.

CEH-39 was expressed using the TNT Quick-Coupled Transcription/Translation system (Promega). Full-length CEH-39 cDNA was cloned into pSG5 (Stratagene), and 1 μ g of plasmids was used per 50- μ L reaction. Protein expression was confirmed using SDS-PAGE/Western blotting. For controls, 1 μ g of empty pSG5 vector was used to prime the reactions.

EMSAs

dsDNA probes of ~300 bp were generated by PCR using oligonucleotides engineered to have unique AgeI sites. Probes were digested with AgeI (New England Biolabs), purified over QiaQuick Gel Extraction columns (Qiagen), and radiolabeled by Klenow polymerase fill-in using 32 P- α -dGTP (3000 Ci/mmol) (PerkinElmer). Labeled double-stranded probes were extracted after PAGE. For each binding reaction, 10 nM final probe concentration (50,000 counts per minute [cpm]) was used in binding buffer 1 [10 mM Tris-Cl at pH 7.5, 2 mM MgCl₂, 250 mM KCl,

5 mg/mL BSA, 100 ng/ μ L poly deoxyinosinic-deoxycytidylic acid [poly(dI-dC)]]. For binding of SEX to the 300-mer probes, binding buffer 1 was supplemented with 160 ng/ μ L poly(dI-dC). For shorter probes, commercially prepared oligonucleotides were synthesized, annealed, and radioactively labeled as above. After labeling, unincorporated nucleotides were removed by separation over a Sephadex G-50 quick-spin column (GE Biosciences). For binding to the shorter probes, 100 nM final probe concentration was used, possessing 250,000 cpm in binding buffer 2 [10 mM Tris-Cl at pH 7.5, 2 mM MgCl₂, 50 mM KCl, 2.5 mg/mL BSA, 20 ng/ μ L poly(dI-dC)].

For probes of all lengths, binding reactions were supplemented with 150 ng of GST or GST-SEA-1 that had been diluted in nuclear extract dilution (NED) buffer (20 mM HEPES at pH 7.9, 10% glycerol, 300 mM KCl, 10 mg/mL BSA, 1 mM DTT), 20 ng of Sf-9 nuclear extract infected with nonrecombinant baculovirus or infected with baculovirus encoding SEX-1 in NED buffer, or 2 μ L of reticulocyte lysate primed with empty vector or primed with a CEH-39 expression vector. Binding reactions were performed for 15 min at room temperature and resolved on a 5% acrylamide (29:1)/0.5 \times TBE gel for 2 h at 180 V. The gel was dried, exposed to a PhosphorImager screen, and analyzed using a Typhoon PhosphorImager (GE Biosciences). To assess CEH-39 binding to 300-mer probes, the amount of protein-bound probe was quantified. To assess SEX-1 binding, the amount of unbound probe remaining per reaction was quantified. For binding to smaller probes, the amount of protein-bound probe was analyzed for all proteins.

DNase I footprinting assay

xol-1 promoter fragments were PCR-amplified and cloned into pUC19 using the restriction endonucleases EcoRI and BamHI and sequenced. The resulting plasmid was first digested with EcoRI (forward strand) or BamHI (reverse strand), treated with calf intestinal phosphatase (New England Biolabs), and phenol/chloroform-extracted. Five micrograms of the purified DNA was labeled with 300 μ Ci 32 P- γ -dATP (MP Biomedicals) using T4 polynucleotide kinase (New England Biolabs), and unincorporated bases were removed with Sephadex G-50. Fragments were digested with BamHI enzyme (forward strand) or EcoRI enzyme (reverse strand), and labeled fragments were PAGE-purified. A DNase I footprinting assay was performed by incubating a 32 P-labeled probe (~1000 cpm) with 2 μ L of nuclear extract dilution buffer; 600 ng of GST or 600 ng, 300 ng, 150 ng, or 75 ng of GST-SEA-1 on ice for 20 min in 5% glycerol; 37.5 mM KCl; 0.5 mM EDTA; 0.5 mM EGTA; 12.5 mM HEPES (pH 7.6); 25 μ g/mL BSA; 0.1 mM PMSF; and 0.5 mM DTT in a total volume of 45 μ L. After incubation, the samples were treated with 2 ng of DPFF grade DNaseI (Worthington) for 1 min at room temperature. The samples were then phenol/chloroform-extracted, ethanol-precipitated, and resolved on an 8% acrylamide/8 M urea sequencing gel in 1 \times TBE buffer. A sequencing ladder was made by treating a sample of the probe with formic acid and piperidine to cleave at A and G residues (Maxam and Gilbert 1977). The DNase I footprinting assay was visualized on a Typhoon PhosphorImager.

SEA-2 in vivo binding assays on xol-1

Array-bearing embryos carrying either the entire *xol-1* promoter, subregions of the promoter, exons, or control sequences lacking *xol-1* (Fig. 4D) were fixed and stained as described (Carmi et al. 1998). Array strains were made by transforming wild-type animals with a mixture of plasmid or PCR products that possess *xol-1* sequence (10 ng/ μ L), pTY1604 (*lacO* repeat; 50 ng/ μ L), pTY1605 (*lacI::gfp*; 50 ng/ μ L), and pPD118.33 (*Pmyo-2::gfp*; 5 ng/ μ L).

Generation and analysis of *xol-1* transgenic strains

xol-1 transgenes lacking XSE- or ASE-binding sites were constructed as described in the Supplemental Material. Numerous transgenic lines were generated for each wild-type or mutant transgene, and quantitative PCR (qPCR) was performed to assess the copy number of the integrated transgenes once they were crossed into *xol-1*(null) hermaphrodites. Transgenes were then crossed into appropriate XSE and ASE mutant backgrounds to analyze the importance of the ASE- and XSE-binding sites in *xol-1* regulation. All transgenic strains were maintained on *xol-1*(RNAi) feeding bacteria to prevent the misregulation of *xol-1* from killing the animals. To determine the viability of the strains, embryos were transferred from RNAi plates to standard NGM plates with OP50 bacteria and grown for two generations prior to assessing the viability of progeny from L4 hermaphrodites.

Acknowledgments

We thank J. Powell for the isolation of *sea-3*; W. Kruesi for assistance in analyzing modENCODE data; the *Caenorhabditis* Genetics Center; the Gene Knockout Consortium, and the National Bioresource Project for strains; T. Cline and B. Wheeler for critical comments on the manuscript; and J. Gardner and D. Stalford for assistance with figures. This work was supported by NIH grant R01-GM30702. B.F. was supported by American Cancer Society Post-doctoral Fellowship PF-06-027-01-DCC, and M.M.J. was supported by NIH training grant T32-GM07127. B.J.M. is an investigator of the Howard Hughes Medical Institute.

References

- Achermann JC, Ito M, Ito M, Hindmarsh PC, Jameson JL. 1999. A mutation in the gene encoding steroidogenic factor-1 causes XY sex reversal and adrenal failure in humans. *Nat Genet* **22**: 125–126.
- Akerib CC, Meyer BJ. 1994. Identification of X chromosome regions in *Caenorhabditis elegans* that contain sex-determination signal elements. *Genetics* **138**: 1105–1125.
- Asahara H, Dutta S, Kao HY, Evans RM, Montminy M. 1999. Pbx-Hox heterodimers recruit coactivator-corepressor complexes in an isoform-specific manner. *Mol Cell Biol* **19**: 8219–8225.
- Baldini A. 2006. The 22q11.2 deletion syndrome: A gene dosage perspective. *ScientificWorldJournal* **6**: 1881–1887.
- Baniahmad A, Ha I, Reinberg D, Tsai S, Tsai MJ, O'Malley BW. 1993. Interaction of human thyroid hormone receptor β with transcription factor TFIIB may mediate target gene derepression and activation by thyroid hormone. *Proc Natl Acad Sci* **90**: 8832–8836.
- Barbash DA, Cline TW. 1995. Genetic and molecular analysis of the autosomal component of the primary sex determination signal of *Drosophila melanogaster*. *Genetics* **141**: 1451–1471.
- Bessereau JL, Wright A, Williams DC, Schuske K, Davis MW, Jorgensen EM. 2001. Mobilization of a *Drosophila* transposon in the *Caenorhabditis elegans* germ line. *Nature* **413**: 70–74.
- Bland ML, Jamieson CA, Akana SF, Bornstein SR, Eisenhofer G, Dallman MF, Ingraham HA. 2000. Haploinsufficiency of steroidogenic factor-1 in mice disrupts adrenal development leading to an impaired stress response. *Proc Natl Acad Sci* **97**: 14488–14493.
- Bridges CB. 1921. Triploid intersexes in *Drosophila Melanogaster*. *Science* **54**: 252–254.
- Bull JJ. 1983. *Evolution of sex determining mechanisms*. The Benjamin/Cummings Publishing Co, Inc., Menlo Park, CA.
- Cai C, He HH, Chen S, Coleman I, Wang H, Fang Z, Chen S, Nelson PS, Liu XS, Brown M, et al. 2011. Androgen receptor gene expression in prostate cancer is directly suppressed by the androgen receptor through recruitment of lysine-specific demethylase 1. *Cancer Cell* **20**: 457–471.
- Carmi I, Kopczynski JB, Meyer BJ. 1998. The nuclear hormone receptor SEX-1 is an X-chromosome signal that determines nematode sex. *Nature* **396**: 168–173.
- Casey ES, O'Reilly MA, Conlon FL, Smith JC. 1998. The T-box transcription factor *Brachyury* regulates expression of eFGF through binding to a non-palindromic response element. *Development* **125**: 3887–3894.
- Charlesworth D, Mank JE. 2010. The birds and the bees and the flowers and the trees: Lessons from genetic mapping of sex determination in plants and animals. *Genetics* **186**: 9–31.
- Chen H, Smit-McBride Z, Lewis S, Sharif M, Privalsky ML. 1993. Nuclear hormone receptors involved in neoplasia: erb A exhibits a novel DNA sequence specificity determined by amino acids outside of the zinc-finger domain. *Mol Cell Biol* **13**: 2366–2376.
- Chuang PT, Albertson DG, Meyer BJ. 1994. DPY-27: A chromosome condensation protein homolog that regulates *C. elegans* dosage compensation through association with the X chromosome. *Cell* **79**: 459–474.
- Cline TW. 1988. Evidence that sisterless-a and sisterless-b are two of several discrete 'numerator elements' of the X/A sex determination signal in *Drosophila* that switch Sxl between two alternative stable expression states. *Genetics* **119**: 829–862.
- Cline TW, Meyer BJ. 1996. Vive la difference: Males vs females in flies vs worms. *Annu Rev Genet* **30**: 637–702.
- Dawes HE, Berlin DS, Lapidus DM, Nusbaum C, Davis TL, Meyer BJ. 1999. Dosage compensation proteins targeted to X chromosomes by a determinant of hermaphrodite fate. *Science* **284**: 1800–1804.
- Erickson JW, Cline TW. 1991. Molecular nature of the *Drosophila* sex determination signal and its link to neurogenesis. *Science* **251**: 1071–1074.
- Erickson JW, Cline TW. 1993. A bZIP protein, *sisterless-a*, collaborates with bHLH transcription factors early in *Drosophila* development to determine sex. *Genes Dev* **7**: 1688–1702.
- Erickson JW, Quintero JJ. 2007. Indirect effects of ploidy suggest X chromosome dose, not the X:A ratio, signals sex in *Drosophila*. *PLoS Biol* **5**: e332.
- Fire A. 1992. Histochemical techniques for locating *Escherichia coli* β -galactosidase activity in transgenic organisms. *Genet Anal Tech Appl* **9**: 151–158.
- Flomen RH, Vatcheva R, Gorman PA, Baptista PR, Groet J, Barisic I, Ligutic I, Nizetic D. 1998. Construction and analysis of a sequence-ready map in 4q25: Rieger syndrome can be caused by haploinsufficiency of RIEG, but also by chromosome breaks approximately 90 kb upstream of this gene. *Genomics* **47**: 409–413.
- Gladden JM, Meyer BJ. 2007. A ONECUT homeodomain protein communicates X chromosome dose to specify *Caenorhabditis elegans* sexual fate by repressing a sex switch gene. *Genetics* **177**: 1621–1637.
- Gladden JM, Farboud B, Meyer BJ. 2007. Revisiting the X:A signal that specifies *Caenorhabditis elegans* sexual fate. *Genetics* **177**: 1639–1654.
- Hargitai B, Kutnyanszky V, Blauwkamp TA, Stetak A, Csankovszki G, Takacs-Vellai K, Vellai T. 2009. *xol-1*, the master sex-switch gene in *C. elegans*, is a transcriptional target of the terminal sex-determining factor TRA-1. *Development* **136**: 3881–3887.
- Herskowitz I. 1989. A regulatory hierarchy for cell specialization in yeast. *Nature* **342**: 749–757.

- Hodgkin J, Zellan JD, Albertson DG. 1994. Identification of a candidate primary sex determination locus, *fox-1*, on the X chromosome of *Caenorhabditis elegans*. *Development* **120**: 3681–3689.
- Huang X, Zhang H, Zhang H. 2011. The zinc-finger protein SEA-2 regulates larval developmental timing and adult lifespan in *C. elegans*. *Development* **138**: 2059–2068.
- Iyaguchi D, Yao M, Watanabe N, Nishihira J, Tanaka I. 2007. DNA recognition mechanism of the ONECUT homeodomain of transcription factor HNF-6. *Structure* **15**: 75–83.
- Kispert A, Herrmann BG. 1993. The *Brachyury* gene encodes a novel DNA binding protein. *EMBO J* **12**: 3211–3220.
- Kwok RP, Lundblad JR, Chrivia JC, Richards JP, Bachinger HP, Brennan RG, Roberts SG, Green MR, Goodman RH. 1994. Nuclear protein CBP is a coactivator for the transcription factor CREB. *Nature* **370**: 223–226.
- Lee DY, Teyssier C, Strahl BD, Stallcup MR. 2005a. Role of protein methylation in regulation of transcription. *Endocr Rev* **26**: 147–170.
- Lee MG, Wynder C, Cooch N, Shiekhattar R. 2005b. An essential role for CoREST in nucleosomal histone 3 lysine 4 demethylation. *Nature* **437**: 432–435.
- Lindsay EA, Vitelli F, Su H, Morishima M, Huynh T, Pramparo T, Jurecic V, Ogunrinu G, Sutherland HF, Scambler PJ, et al. 2001. Tbx1 haploinsufficiency in the DiGeorge syndrome region causes aortic arch defects in mice. *Nature* **410**: 97–101.
- Liu W, Selever J, Lu MF, Martin JF. 2003. Genetic dissection of Pitx2 in craniofacial development uncovers new functions in branchial arch morphogenesis, late aspects of tooth morphogenesis and cell migration. *Development* **130**: 6375–6385.
- Ludewig AH, Kober-Eisermann C, Weitzel C, Bethke A, Neubert K, Gerisch B, Hutter H, Antebi A. 2004. A novel nuclear receptor/coregulator complex controls *C. elegans* lipid metabolism, larval development, and aging. *Genes Dev* **18**: 2120–2133.
- Luz JG, Hassig CA, Pickle C, Godzik A, Meyer BJ, Wilson IA. 2003. XOL-1, primary determinant of sexual fate in *C. elegans*, is a GHMP kinase family member and a structural prototype for a class of developmental regulators. *Genes Dev* **17**: 977–990.
- Madl JE, Herman RK. 1979. Polyploids and sex determination in *Caenorhabditis elegans*. *Genetics* **93**: 393–402.
- Maira M, Couture C, Le Martelot G, Pulichino AM, Bilodeau S, Drouin J. 2003. The T-box factor Tpit recruits SRC/p160 co-activators and mediates hormone action. *J Biol Chem* **278**: 46523–46532.
- Mangelsdorf DJ, Thummel C, Beato M, Herrlich P, Schutz G, Umesono K, Blumberg B, Kastner P, Mark M, Chambon P, et al. 1995. The nuclear receptor superfamily: The second decade. *Cell* **83**: 835–839.
- Maxam AM, Gilbert W. 1977. A new method for sequencing DNA. *Proc Natl Acad Sci* **74**: 560–564.
- Meyer BJ. 2010. Targeting X chromosomes for repression. *Curr Opin Genet Dev* **20**: 179–189.
- Michelitsch MD, Weissman JS. 2000. A census of glutamine/asparagine-rich regions: Implications for their conserved function and the prediction of novel prions. *Proc Natl Acad Sci* **97**: 11910–11915.
- Miller LM, Plenefisch JD, Casson LP, Meyer BJ. 1988. *xol-1*: A gene that controls the male modes of both sex determination and X chromosome dosage compensation in *C. elegans*. *Cell* **55**: 167–183.
- Mori AD, Bruneau BG. 2004. TBX5 mutations and congenital heart disease: Holt-Oram syndrome revealed. *Curr Opin Cardiol* **19**: 211–215.
- Murakami M, Nakagawa M, Olson EN, Nakagawa O. 2005. A WW domain protein TAZ is a critical coactivator for TBX5, a transcription factor implicated in Holt-Oram syndrome. *Proc Natl Acad Sci* **102**: 18034–18039.
- Muscat GE, Burke LJ, Downes M. 1998. The corepressor N-CoR and its variants RIP13a and RIP13Δ1 directly interact with the basal transcription factors TFIIB, TAFII32 and TAFII70. *Nucleic Acids Res* **26**: 2899–2907.
- Nicoll M, Akerib CC, Meyer BJ. 1997. X-chromosome-counting mechanisms that determine nematode sex. *Nature* **388**: 200–204.
- Nigon V. 1951. Polyploidie experimentale chez un nematode libre, *Rhabditis elegans* Maupas. *Bull Biol Fr Belg* **85**: 187–225.
- Perry MW, Cande JD, Boettiger AN, Levine M. 2009. Evolution of insect dorsoventral patterning mechanisms. *Cold Spring Harb Symp Quant Biol* **74**: 275–279.
- Pferdehirt RR, Kruesi WS, Meyer BJ. 2011. An MLL/COMPASS subunit functions in the *C. elegans* dosage compensation complex to target X chromosomes for transcriptional regulation of gene expression. *Genes Dev* **25**: 499–515.
- Powell JR, Jow MM, Meyer BJ. 2005. The T-box transcription factor SEA-1 is an autosomal element of the X:A signal that determines *C. elegans* sex. *Dev Cell* **9**: 339–349.
- Privalsky ML. 2004. The role of corepressors in transcriptional regulation by nuclear hormone receptors. *Annu Rev Physiol* **66**: 315–360.
- Rhind NR, Miller LM, Kopczynski JB, Meyer BJ. 1995. *xol-1* acts as an early switch in the *C. elegans* male/hermaphrodite decision. *Cell* **80**: 71–82.
- Rosenfeld MG, Lunyak VV, Glass CK. 2006. Sensors and signals: A coactivator/corepressor/epigenetic code for integrating signal-dependent programs of transcriptional response. *Genes Dev* **20**: 1405–1428.
- Salz HK, Erickson JW. 2010. Sex determination in *Drosophila*: The view from the top. *Fly (Austin)* **4**: 60–70.
- Sefton L, Timmer JR, Zhang Y, Beranger F, Cline TW. 2000. An extracellular activator of the *Drosophila* JAK/STAT pathway is a sex-determination signal element. *Nature* **405**: 970–973.
- Shilo BZ, Haskel-Ittah M, Ben-Zvi D, Schejter ED, Barkai N. 2013. Creating gradients by morphogen shuttling. *Trends Genet* doi: 10.1016/j.tig.2013.01.001.
- Skipper M, Milne CA, Hodgkin J. 1999. Genetic and molecular analysis of *fox-1*, a numerator element involved in *Caenorhabditis elegans* primary sex determination. *Genetics* **151**: 617–631.
- Smith DB, Johnson KS. 1988. Single-step purification of polypeptides expressed in *Escherichia coli* as fusions with glutathione S-transferase. *Gene* **67**: 31–40.
- Williams DC, Boulton T, Ruaud AF, Jorgensen EM, Bessereau JL. 2005. Characterization of *Mos1*-mediated mutagenesis in *Caenorhabditis elegans*: A method for the rapid identification of mutated genes. *Genetics* **169**: 1779–1785.
- Wolfe SA, Nekudova L, Pabo CO. 2000. DNA recognition by Cys2His2 zinc finger proteins. *Annu Rev Biophys Biomol Struct* **29**: 183–212.
- Wong CW, Privalsky ML. 1998. Transcriptional repression by the SMRT-mSin3 corepressor: Multiple interactions, multiple mechanisms, and a potential role for TFIIB. *Mol Cell Biol* **18**: 5500–5510.
- Yao TP, Ku G, Zhou N, Scully R, Livingston DM. 1996. The nuclear hormone receptor coactivator SRC-1 is a specific target of p300. *Proc Natl Acad Sci* **93**: 10626–10631.